In the present, we demonstrate that inhibition of NF-κB activity by ritonavir results in marked increase of apoptosis and induce cell-cycle arrest in EBV-positive lymphoblastoid B cells. We found that ritonavir also suppresses the expression of genes involved in antiapoptosis and cell-cycle progression. In addition, we established preclinical models using newly developed NOD/SCID/γc^{null} (NOG) mouse,[16] a unique type of animal, lacking T-, B- and NK-cells to evaluate the efficacy of antitumor and anti-NF-κB therapies. In the murine model, ritonavir at the clinically relevant dose potently inhibited the growth and infiltration of EBV-transformed LCL cells.

Material and methods

Mice and cells

NOG mice were obtained from the Central Institute for Experimental Animals (Kawasaki, Japan). All mice were maintained under specific-pathogen-free conditions in the Animal Center of Tokyo Medical and Dental University (Tokyo, Japan). The Ethical Review Committee of the Institute approved the experimental protocol.

EBV-positive immortalized lymphoblatoid B-cell lines (LCL-Ya, LCL-Ao, LCL-Ka and LCL-Ku) were cultured in RPMI 1640 medium supplemented with 10% heat-inactivated fetal bovine serum (JRH Biosciences, Lenexa, KS), 100 U/ml penicillin, and 10 μg/ml streptomycin. Peripheral blood mononuclear cells (PBMCs) from 3 healthy volunteers were analyzed. Mononuclear cells were isolated by Ficoll-Paque density gradient centrifugation (GE Healthcare Biosciences, Uppsala, Sweden) and washed with PBS.

Cell viability assay

The effect of ritonavir on cell viability of LCLs and PBMCs from healthy donors was examined by the reagent, water-soluble tetrazolium (WST)-8 (Wako Chemicals, Osaka, Japan). Briefly, 2×10^5 cells were incubated in a 96-well microculture plate in the absence or presence of various concentrations of ritonavir. After 72 hr of culture, WST-8 (5 μl) was added for the last 4 hr of incubation and absorbance at 450 nm was measured using an automated microplate reader. Measurement of mitochondrial dehydrogenase cleavage of WST-8 to formazan dye provides an indication of the level of cell viability.

Cell-cycle analysis

Cells were plated at a density of 3×10^5/ml in 60-mm tissue culture dishes. Twelve hours after plating, cells were exposed to 40 μM ritonavir for 24 h. Cell-cycle analysis was performed with the CycleTEST PLUS DNA reagent kit (Becton Dickinson, San Jose, CA). Briefly, cells were washed with a buffer solution containing sodium citrate, sucrose and dimethyl sulfoxide, suspended in a solution containing RNase A, and stained with 125 μg/ml propidium iodide (PI) for 10 min. Cell suspensions were analyzed on EPICS XL flow cytometer (Beckman Coulter, Fullerton, CA) using EXPO32 software. The cell population at each cell-cycle phase was determined with MultiCycle software (Beckman Coulter).

Assay for apoptosis

Cells were plated at a density of 3×10^5/ml in 60-mm tissue culture dishes. Twelve hours after plating, cells were exposed to ritonavir for 72 hr. Apoptosis was quantified by double staining with Annexin-V-Fluos (Roche Diagnostics, Mannheim, Germany) and PI (Backman Coulter) according to the instructions supplied by the manufacturer. Cells were analyzed on EPICS XL flow cytometer (Beckman Coulter) using EXPO32 software.

Western blot analysis

Treated cells were solubilized at 4°C in lysis buffer containing 62.5 mM Tris-HCl (pH 6.8), 2% SDS, 10% glycerol, 6% 2-mercaptoethanol and 0.01% bromophenol blue. Samples were subjected to electrophoresis on SDS-polyacrylamide gels followed by transfer to a polyvinylidine difluoride membrane and probing with the following specific antibodies: polyclonal antibodies against survivin, cyclin D2 (Santa Cruz Biotechnology, Santa Cruz, CA), Bcl-X_L (BD Transduction Laboratories, San Jose, CA) and monoclonal antibodies against Bcl-2, p53, actin (NeoMarkers, Fremont, CA), PARP (BD Transduction Laboratories) and LMP-1 (DAKO, Kyoto, Japan). The protein bands recognized by the antibodies were visualized using the enhanced chemiluminescence system (Amersham, Piscataway, NJ).

Electrophoresis mobility shift assay (EMSA)

Cells were placed in culture at 1×10^6 cells/ml and examined for inhibition of NF-κB 24 hr after exposure to ritonavir. Nuclear proteins were extracted, and NF-κB binding activities to κB element were examined by EMSA as described previously.[8] In brief, 5 μg of nuclear extracts were preincubated in a binding buffer containing 1 μg of poly (dI:dC) (Amersham Biosciences), followed by addition of ^{32}P-labeled oligonucleotide probe containing NF-κB element (5×10^4 c.p.m.). These mixtures were incubated for 15 min at room temperature. The DNA-protein complexes were separated on a 4% polyacrylamide gel and visualized by autoradiography. To examine the specificity of the NF-κB element probe, unlabeled competitor oligonucleotides were preincubated with nuclear extracts for 15 min before incubation with probes. The probe or competitors used were prepared by annealing the sense and antisense synthetic oligonucleotides as follows: a typical NF-κB element from the *IL-2Rα* gene, 5′-gatcCGGCAGGGGAATCTCCCTCTC-3′; and AP-1 element of the *IL-8* gene, 5′-gactGTGATGACTCAGGTT-3′. Underlined sequences represent the NF-κB or AP-1 binding site. To identify NF-κB protein in the DNA protein complex revealed by EMSA, we used antibodies specific for various NF-κB proteins, including p50, p65, c-Rel, RelB and p52 (Santa Cruz Biotechnology), to elicit a supershift DNA protein complex formation. These antibodies were incubated with the nuclear extracts for 45 min at room temperature before incubation with radiolabeled probes.

Inoculation of EBV-positive immortalized LCLs and collection of samples

LCL Cells [LCL-Ya, LCL-Ao, LCL-Ka and LCL-Ku] were washed twice with serum-free RPMI-1640 medium and resuspended in same medium. Mice were anaesthetized with ether and cells were inoculated subcutaneously (sc) in the postauricular region of NOG mice at a dose of 1×10^7 cells per mouse. All mice were sacrificed 3 weeks after inoculation with lymphoma cells. We measured tumor size 3 weeks after inoculation. Tissues and various organs of mice were collected and fixed with Streck Tissue Fixative, then processed to paraffin wax-embedded sections for staining with hematoxylin and eosin (HE) and immunostaining.

PCR primer and conditions

Detection of the BamHI W repeat region of the EBV genome was performed using 100 ng of genomic DNA extracted from LCLs as follows. LCLs were lysed with genomic DNA extraction buffer (100 mM Tris-HCl pH8.0, 5 mM EDTA, 0.2% SDS, 200 mM NaCl and 200 μg/mL proteinase K) and the lysate was incubated at 50°C for 3 hr. After phenol-chloroform extraction, genomic DNA was purified by ethanol precipitation procedure. A 121-bp fragment of the EBV W repeat region was amplified by the forward primer 5′-CGCATAATGGCGGACCTAG-3′ and reverse primer 5′-CAAACAAGCCCACTCCCC-3′ in a 25 μl reaction mixture comprising 1 × AmpliTaq Gold buffer, 3.5 mM MgCl2, 200 μM dNTP, 300 nM primers, 200 nM probe and 0.025 U/μl AmpliTaq Gold. The PCR cycle conditions were as follows: a DNA denaturation and polymerase activation step of 10 min at 95°C and then 40 cycles of amplification (95°C for 15 sec, 60°C for 1 min). PCR products were separated by electrophoresis on agarose gels, stained with ethidium bromide and visualized by UV-light.

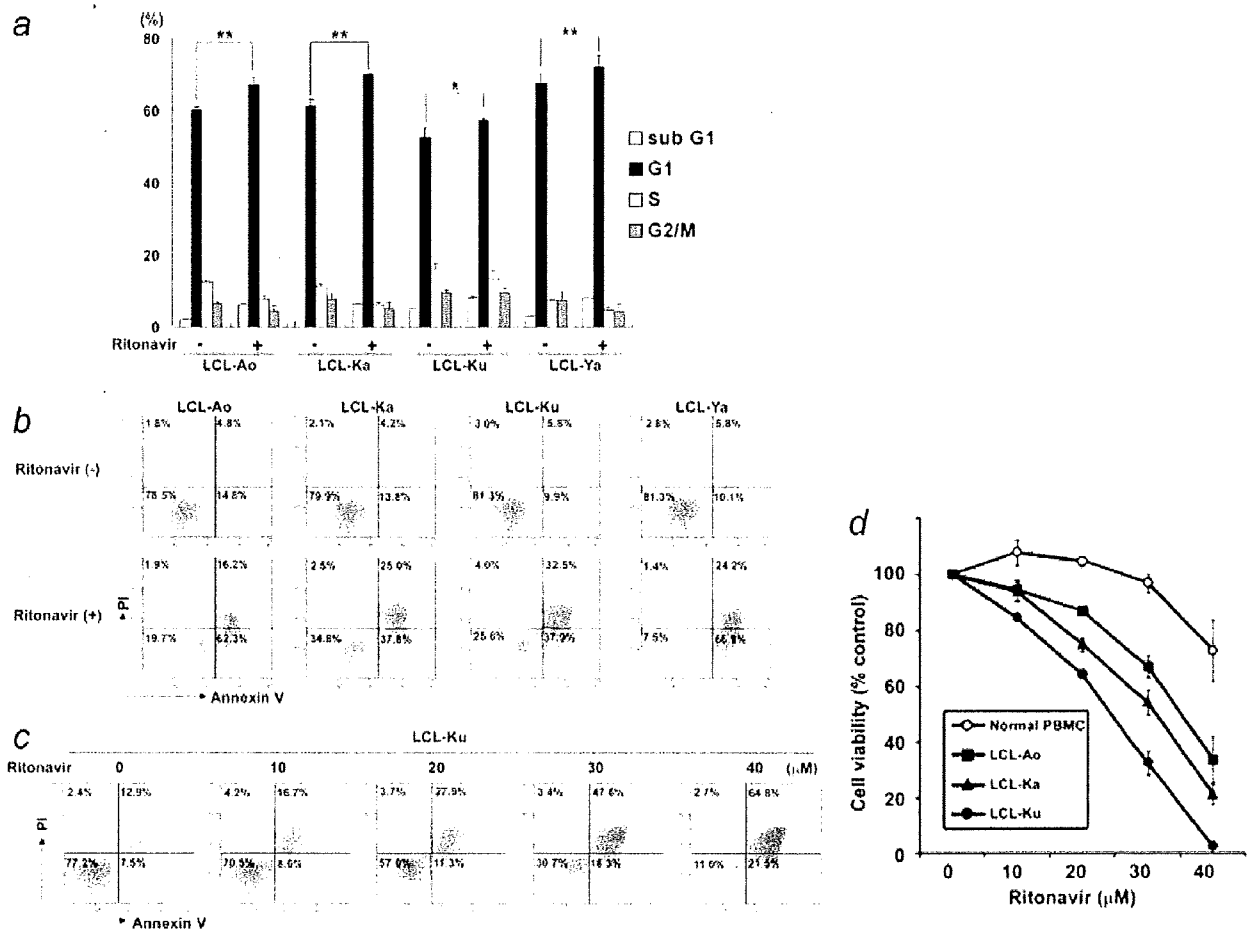

FIGURE 1 – Effect of ritonavir on cell cycle arrest and induction of apoptosis of EBV-positive lymphoblastoid B cells. (*a*) Effect of ritonavir on cell cycle progression of EBV-positive lymphoblastoid B cells. Cells were cultured for 24 hr with (+) or without (−) ritonavir (40 μM). DNA content was analyzed by flow cytometry with PI staining. Sub G_1, S and G_2/M indicate the stages of the cell cycle. Data are expressed as the mean percentages of the cells from three independent experements. Significance of differences between % G_1 of ritonavir treated (+) and untreated (−) cells calculated by Student's *t*-test is shown as *P*-value with astalisk(s). $*p < 0.05$ and $**p < 0.01$. (*b*) Effect of ritonavir on induction of apoptosis of EBV-immortalized B-cell lines. Cells were cultured for 72 hr with (+) or without (−) ritonavir (40 μM). (*c*) Ritonavir induces apoptosis of EBV-immortalized B-cell lines in a dose-dependent manner. LCL-Ku cells were cultured for 72 hr with increasing concentration of ritonavir (0, 10, 20, 30, 40 μM). Cells were harvested and stained with Annexin-V and PI. Apoptosis was analyzed by flow cytometry. Bottom left quadrants, viable cells; bottom right quadrants, early apoptotic cells. Top right quadrants, nonviable, late apoptotic/necrotic cells. (*d*) Effect of ritonavir on cell viability of LCLs and PBMCs from normal healthy controls. LCLs and PBMCs were incubated in the presence of various concentrations of ritonavir for 72 hr and viability of the cultured cells was measured by WST-8 assay. Relative viability of the cultured cells is presented as the mean determined on LCLs and PBMCs from triplicate cultures. A relative viability of 100% was designated as total number of cells that grew in 72-hr cultures in the absence of ritonavir.

Treatment of tumor-bearing mice with ritonavir

Ritonavir was obtained from Abbott Labs, North Chicago, IL. LCL-Ku cells (1×10^7) were inoculated s.c. in the post-auricular region of NOG mice. The drug was administered s.c. into the tumor cells inoculated site of mice at doses of 30 mg/kg/day, beginning on day 0 for 3 weeks. The control mice received RPMI-1640 (200 μl) simultaneously. In other experiments, ritonavir or RPMI-1640 was also administered intraperitoneally into mice as the same doses stated above, beginning on day 4 for 18 days.

In situ *hybridization*

EBERs were detected by *in situ* hybridization using fluorescein isothiocyanate (FITC)-conjugated EBER PNA (peptide nucleic acid)-probe (DAKO). Briefly, formalin-fixed, paraffin-embedded tissue sections of tumor and various organs were deparaffinized and hydrated in xylenes and graded alcohol series, then rinsed for 5 min in PBS. Deparaffinized samples were incubated with 10 ng/μl of proteinase K for 20 min at 37°C followed by washing, and then incubated with 0.3% methanol for 30 min at room temperature. After washing in PBS, the sections were hybridized with FITC-conjugated EBER-PNA probe in the hybridization solution for 90 min at 56°C. The slides were washed twice in 0.2 × SSC for 20 min at 56°C, and incubated with anti-FITC monoclonal antibody (DAKO) for 45 min at 37°C. Followed by washing, the slides were incubated with horse-radish peroxidase-conjugated polymer reagent (Envision, DAKO) for 30 min at room temperature. Positive staining was visualized after incubation of these samples with a mixture of 0.05% 3,3′-diaminobenzidine tetrahydrochloride in 50 mM Tris-HCl buffer pH7.6 and 0.01% hydrogen peroxide for 5 min. The samples were counterstained with hematoxlin for 2 min, hydrated completely, cleaned in xylene and then mounted. The samples were visualized and photographed under light microscopy (BX41 and DP70; Olympus, Tokyo, Japan).

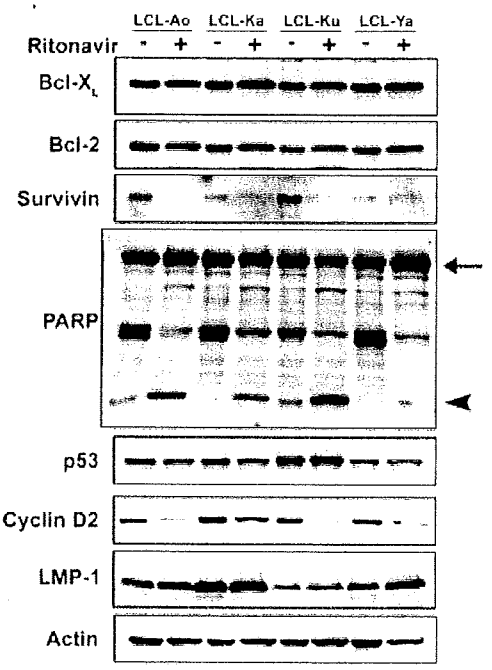

FIGURE 2 – Ritonavir inhibits expression of apoptosis- and cell cycle-associated proteins. EBV-immortalized B-cell lines were cultured with (+) or without (−) ritonavir (40 μM) for 24 hr. Cells were harvested and subjected to Western blot analysis. The polyvinylidene fluoride membrane was sequentially probed with indicated antibodies. Arrow indicates full-length PARP (116 kDa) and arrow head indicates cleaved form of PARP (25 kDa). Essentially the same results were obtained in 3 experiments and representative data are shown.

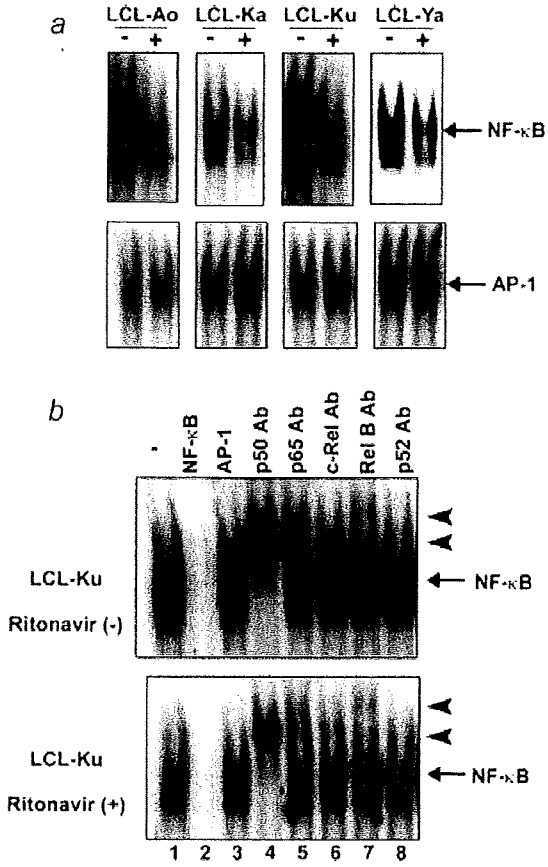

FIGURE 3 – Ritonavir inhibits constitutive NF-κB activation. (*a*) EBV-immortalized B-cell lines were cultured with (+) or without (−) ritonavir (40 μM) for 24 hr and assessed for NF-κB and AP-1-DNA binding activity. (*b*) Cold competition using 100-fold excess of unlabeled NF-κB oligonucleotide, or AP-1 oligonucleotide (lanes 2–3) demonstrated the specificity of the protein/DNA binding complexes. Specificity of NF-κB binding was also determined by using antibodies to the NF-κB components p50, p65, c-Rel, RelB and p52, resulting in supershift (lanes 4–8). Arrows indicate specific complexes of NF-κB with wild type NF-κB oligonucleotide. Arrow heads indicate supershift. Essentially the same results were obtained in 3 experiments and representative data are shown.

Results

Ritonavir induces cell-cycle arrest and apoptosis of LCLs

Ritonavir was examined for its effect on cell-cycle distribution of EBV-immortalized LCLs (Fig. 1*a*). Ritonavir effectively inhibited cell-cycle progression, as evidenced by increased proportion of the cells in G_1 phase of LCL-Ao, LCL-Ka, LCL-Ku and LCL-Ya (LCL-Ao: from 60.1% to 67.1%; LCL-Ka: from 61.2% to 69.9%; LCL-Ku: from 52.6% to 57.3%; and LCL-Ya: from 67.4% to 72.1%). These results indicated that ritonavir induced cell-cycle arrest at G_1-phase. The weak accumulation of cells in G_1 phase by ritonavir suggests that it might rather be an apoptosis inducer than a cell growth inhibitor.

Furthermore, we evaluated the effect of ritonavir on the cell viability of LCLs and PBMCs from healthy individuals (Fig. 1*d*). Ritonavir effectively reduced the survival of LCLs (LCL-Ao, LCL-Ka and LCL-Ku) as measured by WST-8 on the third day of culture in a dose-dependent manner. In contrast, ritonavir hardly affected the survival of PBMCs from healthy volunteers.

The effect of ritonavir on apoptosis was examined by the Annexin-V and PI method. Annexin-V binds to the cells that express phosphatidylserine on the outer layer of the cell membrane, a characteristic feature of cells entering apoptosis. Early apoptotic cells were stained with Annexin V but not with PI. Late apoptotic and necrotic cells were stained with both fluorescent. Ritonavir induced increased proportion of cells positive for Annexin-V and negative for PI in all cell lines (LCL-Ao: from 14.8% to 62.3%; LCL-Ka: from 13.8% to 37.8%; LCL-Ku: from 9.9% to 37.9% and LCL-Ya: from 10.1% to 66.9%) (Fig. 1*b*). Ritonavir also induced dose-dependent increasing of Annexin-V positive and PI negative cells in LCL-Ku cells (Fig. 1*c*), indicating increasing apoptosis of ritonavir-treated cells.

Ritonavir down-regulates the expression of the cell-cycle- and apoptosis-associated genes

The antiproliferative and proapoptotic effects of ritonavir were explored by examining the levels of intracellular regulators of cell-cycle and apoptosis after exposure to ritonavir (Fig. 2). Ritonavir down-regulated the levels of survivin and cyclin D2 in EBV-immortalized B-cell lines. We also observed increased cleavage of PARP in these cells. However, ritonavir did not modulate the other regulators of cell-cycle and apoptosis such as Bcl-X_L, Bcl-2 and p53. Ritonavir had no effect on the expression of viral proteins such as LMP-1, suggesting that ritonavir may induce cell-cycle arrest and apoptosis by down-regulating the levels of survivin and cyclin D2 without reducing the virus levels in the cells.

Ritonavir suppresses constitutive NF-κB expressed by EBV-transformed LCLs

To examine the effect of ritonavir on NF-κB DNA binding, EMSA was performed. EBV-immortalized B-cell lines were incubated with or without 40 μM ritonavir for 24 h, and nuclear extracts were prepared and examined for NF-κB by EMSA.

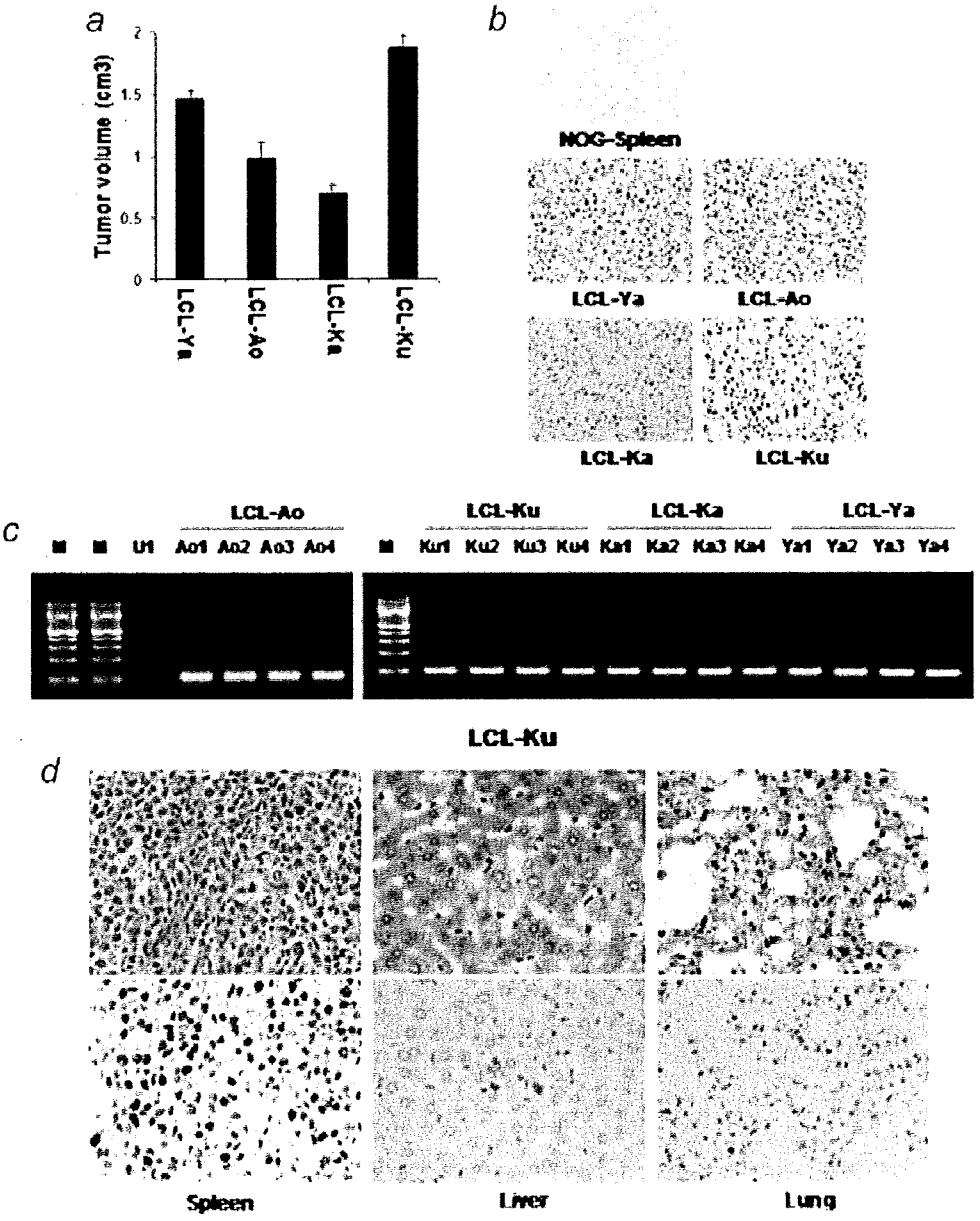

FIGURE 4 – Successful engraftment and infiltration of EBV-positive lymphoblastoid B cells in NOG mice. (*a*) Subcutaneous tumor size in mice 21 days after inoculation with various LCL cells. (*b*) *In situ* hybridization for EBER of spleen from NOG mice not receiving tumor cells, as a negative control and tumor tissues of LCL cells injected mice. Magnification ×40. (*c*) Detection of viral DNA by PCR. M, Marker; U1; EBV-negative U937 cell for negative control; Ao1, *in vitro* culture and Ao2, Ao3 and Ao4, *in vivo* samples from 3 different mice inoculated with LCL-Ao; Ku1, *in vitro* culture and Ku2, Ku3 and Ku4, *in vivo* sample from 3 different mice inoculated with LCL-Ku; Ka1, *in vitro* culture and Ka2, Ka3 and Ka4, *in vivo* sample from 3 different mice inoculated with LCL-Ka, Ya1, *in vitro* culture and Ya2, Ya3 and Ya4, *in vivo* sample from 3 different mice inoculated with. LCL-Ya. Infiltration of EBV-immortalized B-cell lines in various organs of NOG mice. (*d*) HE and *in situ* hybridization for EBER of spleen, liver and lung of mice inoculated with LCL-Ku cells. Left, middle and right panels represent spleen, liver and lung, respectively. Upper and lower panels represent HE and EBER, respectively (magnification ×40).

Down-regulation of NF-κB occurred in all cell lines (Fig. 3*a*, upper panels). Inhibition appeared specific to NF-κB, because no significant change in binding activity of AP-1 was observed after treatment of cells with ritonavir (Fig. 3*a*, lower panels). Also, the observed protein/DNA binding was specific for NF-κB, because the binding was effectively competed and abrogated by excess unlabeled NF-κB oligonucleotide but not by mutant NF-κB or AP-1 oligonucleotide (Fig. 3*b*). LCL-Ku cell extract without ritonavir treatment contained p50, p65 and Rel B proteins in the NF-κB complex (Fig. 3*b*, upper panel), and ritonavir did not affect components of the NF-κB complex (Fig. 3*b*, lower panel).

Efficient engraftment and infiltration of EBV-transformed LCLs in NOG mice

EBV-immortalized LCLs (LCL-Ya, LCL-Ao, LCL-Ka and LCL-Ku) were inoculated s.c. in the post-auricular region of NOG mice (Fig. 4 and Table I). Mice inoculated with LCL cells (LCL-

TABLE I – *IN VIVO* CHARATERISTICS OF EBV-POSITIVE LYMPHOBLASTOID B CELLS IN NOG MICE

Cell line	Orgin/EBV status	No. of cells inoculated/mouse (10^7)[1]	Inoculation route[2]	Day of sacrifice after inoculation	No. of mice with tumor/no. of mice inoculated[3]	Organ-infiltration[4]		
						Spleen	Liver	Lung
LCL-Ya	B/+	1	sc	21	03/03	++	–	–
LCL-Ao	B/+	1	sc	21	03/03	++	–	–
LCL-Ka	B/+	1	sc	21	03/03	++	–	–
LCL-Ku	B/+	1	sc	21	21/21	+++	+	+

[1]Mice were inoculated with 1×10^7 cells per mouse.–[2]sc, subcutaneous.–[3]Number of animals in which tumor developed.–[4]Organ-infiltration was examined by histological analysis.–, no infiltration; +, slight infiltration; ++, marked infiltration; +++, massive infiltration.

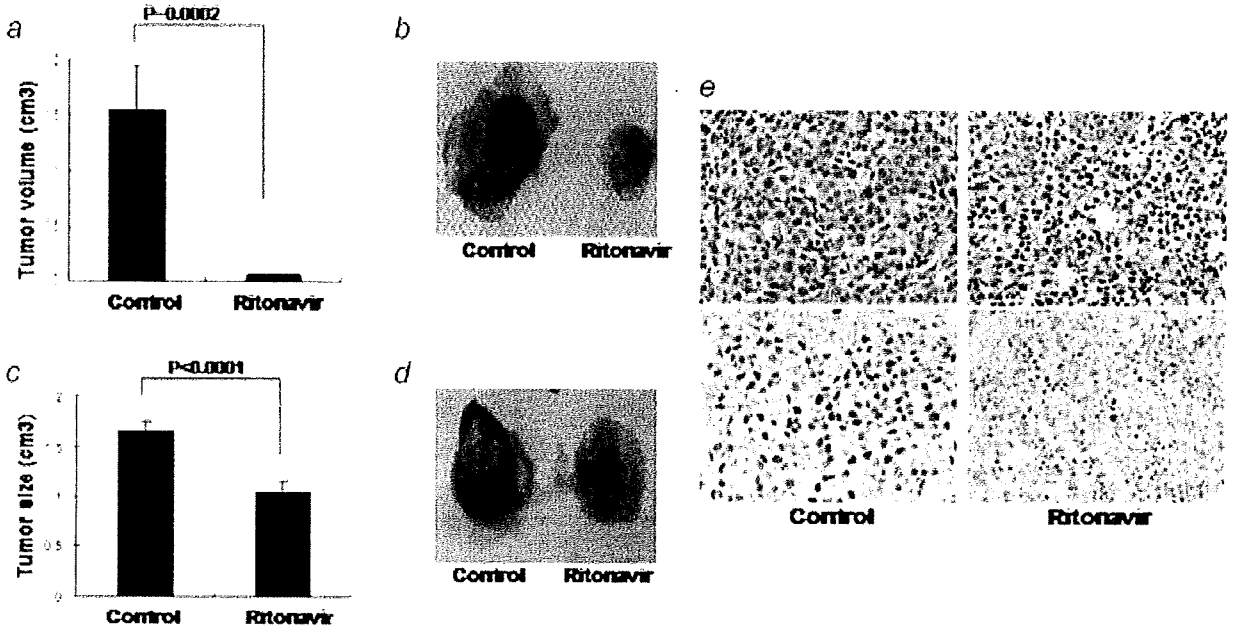

FIGURE 5 – Effect of ritonavir on lymphoma cell growth and infiltration. Mice were injected with LCL-Ku cells (1×10^7 cells) s.c. in the postauricular region. (*a* and *b*) The drug was administered s.c. into the tumor cells inoculated site of mice at doses of 30 mg/kg/day, beginning on day 0 for 3 weeks. The control mice received RPMI-1640 (200 µl) simultaneously. (*a*) Average size of tumor, data represent the mean ± SD from 6 mice. (*b*) Photograph of subcutaneously formed excised tumor without (left) and with (right) ritonavir treatment. (*c* and *d*) Effect of ritonavir on established tumor, ritonavir or RPMI-1640 was also administered intraperitoneally into mice as the same doses stated above, beginning on day 4 for 18 days. (*c*) Average size of tumor, data represent the mean ± SD from 6 mice. (*d*) Photograph of subcutaneously formed excised tumor without (left) and with (right) ritonavir treatment. (*e*) HE and *in situ* hybridization for EBER in spleen tissue of LCL cells injected mice. Magnification ×40. Upper and lower panels show HE and EBER staining, respectively.

Ya, LCL-Ao, LCL-Ka and LCL-Ku) produced a visible tumor within 3 weeks in all NOG mice. LCL-Ku cell was very efficient in the formation of a large tumor (Fig. 4*a*), as well as development of clinical signs of near-death, such as pilorection, weight loss and cachexia in mice at the time point of sacrifice. The average tumor size (LCL-Ya, LCL-Ao, LCL-Ka and LCL-Ku) in NOG mice inoculated s.c. with lymphoma cells was shown in Figure 4*a*. To test whether tumors maintain original histomorphology and expression patterns of tumor markers in NOG, we performed HE and *in situ* hybridization for EBER of normal mice spleen not receiving tumor cells and tumor tissues obtained from mice inoculated with LCLs. Histological analysis revealed that morphologically immunoblastic cells with large nucleus, clear nuclear membrane and broad cytoplasm expressed EBER, whereas EBER was not detected in spleen tissue collected from mice not receiving tumor cells, suggesting that *in vivo* tumor cells preserved well morphology as well as expressed viral gene EBER (Fig. 4*b*). Tumor cells from mice inoculated with EBV-immortalized B-cell lines were positive for DNA of EBV by PCR (Fig. 4*c*). These results showed that EBV-immortalized B-cell lines inoculated s.c. into the postauricular region of NOG mice were able to produce a visible tumor very efficiently. To assess the tissue distribution of lymphoma cells, we carried out histological examinations of the different organs of NOG mice after inoculation of the cells. Proliferation and infiltration of tumor cells were found not only in primary tumor tissues but also in spleen and to a lesser extent in liver and lung of NOG mice inoculated with tumor cells (Table I). HE and *in situ* hybridization staining for EBER showed a degree of infiltration of tumor cells at the site of inoculation and various organs with lymphoma cells (Fig. 4*d*). Interestingly, LCL-Ku cells appeared to infiltrate in various organs of mice more aggressively and massively than other cells. This extremely rapid tumor formation and infiltration in all mice is one of the hallmarks of our clinically relevant animal model without change of histomorphology or tumor marker expression.

Ritonavir suppresses the LCLs growth and infiltration in vivo

To determine the effect of ritonavir on tumor growth and infiltration, we injected LCL-Ku cells (1×10^7) s.c. into the postauricular region of NOG mice. Mice were treated with either RPMI-1640 (as control) or ritonavir (30 mg/kg/day), beginning on either day 0 or day 4. A significant decrease in the size of tumors in mice treated with ritonavir was demonstrated when compared with controls 3 weeks after the injection of tumor cells (Fig. 5*a*). Gross appearance of the mice treated by ritonavir showed apparent

reduction of the tumor mass at 3 weeks after inoculation of tumor cells (Fig. 5*b*). Ritonavir also inhibited the size and growth of established tumors (Fig. 5*c* and 5*d*). Ritonavir at this treatment dosage (30 mg/kg/day for 3 weeks) is well tolerated without adverse findings such as standing of hair, weight loss and cachexia of treated mice, all of which are signs of near death. Clinical evaluation of organ invasion 3 weeks after injection of tumor cells showed that ritonavir treatment inhibited their infiltration into spleen (Fig. 5*e*). In contrast, all control mice showed infiltration with tumor cells into spleen. Organ infiltration of lymphoma cells were analyzed and evaluated by HE and *in situ* hybridization of EBER. Together, these data indicate that ritonavir significantly inhibits lymphoma cell growth and infiltration in various organs of NOG mice (Fig. 5).These results suggest that ritonavir contributes to the reduction of the tumor growth and inhibits the organ infiltration in the mice through targeting the constitutive NF-κB activity.

Discussion

EBV-positive malignancies in immunocompromised patients are associated with high mortality and reduce overall survival period. The various chemotherapies so far developed have not increased significantly the survival of patients with EBV-associated malignancies in immunocompromised patients. Given disappointing results using conventional chemotherapy, new treatment strategies that specially target EBV-transformed cells are need.[1,2] LMP-1 is an oncogene that constitutively activates NF-κB to induce B cell proliferation.[7] It has been previously reported that suppression of high NF-κB activity inhibited cell growth and induced apoptosis of cancer cells as well as EBV-transformed cells both *in vitro* and *in vivo*.[12–20,33] Ritonavir is cytotoxic for different types of malignant cells *in vitro* through affecting proteasomal proteolysis, although concentrations necessary to show the *in vitro* effect exceed the achievable therapeutic drugs level.[27,29,30] It may affect the stabilization of p21, p27 and p53 proteins. Recently, ritonavir has been shown to inhibit NF-κB activity and induce the apoptosis of ATL cells.[20] This led us to investigate whether this drug exhibits anti-tumor effects against EBV-transformed cells *in vitro* and in our preclinical murine model. In the present study, we established a unique murine model that presents aggressive features concerning cell growth and infiltration in SCID mice within 3 weeks. Thus, it represents a novel model to evaluate tissue toxicity and the efficacy of therapeutic agents directed toward the treatment of EBV-associated lymphoproliferative diseases.

The blood-plasma ritonavir concentrations obtained in the therapy of HIV-infection are between 5 to 15 μM,[34] but much higher maximal concentrations (up to 46 μM) have been demonstrated in individual patients.[35] In the present study, we used the concentration of ritonavir for doing *in vitro* experiments from 0 to 40 μM and *in vivo* 30 mg/kg/day used for treatment of AIDS patients. Constitutive and strong NF-κB activation was reported to be a characteristic of LCL and important for LCL growth and survival.[7] Our results indicate that inhibition of NF-κB activity by ritonavir reduced cell growth and induced apoptosis of these cells. This is consistent with down-modulation of NF-κB regulated genes such as antiapoptotic and cell-cycle related genes. Our murine model clearly indicate that 30 mg/kg/day of ritonavir (the same dose used clinically for treating HIV/AIDS patients) significantly inhibits EBV-transformed cell growth and infiltration into various organs of NOG mice. The plasma exposure produced by this dose in mice is only approximately one-half of the plasma exposure observed with the licensed dose of ritonavir in human (600 mg BID). In our murine model, ritonavir at this treatment dosage is well tolerated without severe adverse effects observed in the mice during the treatment period. These data strongly suggest that the HIV protease inhibitor, ritonavir, is a promising antitumor agent against EBV-transformed cells and could be used clinically for treatment of EBV-associated malignancies. These results suggest that anti-tumor activity of ritonavir correlates with suppression of NF-κB activity.

In summary, we have established a novel NOG EBV-associated lymphoma model that presents features similar to patients with EBV-infection in immunocompromised patients. These results also indicate that the HIV protease inhibitor, ritonavir, showed antitumor and anti-NF-κB activity against EBV-transformed cells. Finally, our results strongly suggest that NF-κB serves as a potential molecular target to treat EBV-associated malignancies, and that ritonavir might be used clinically as a single compound or in combination with the reducing dose of chemotherapeutic agents for treatment of patients with life-threatening EBV-associated lymphoproliferative diseases and AIDS-associated lymphomas.

Acknowledgements

We thank D. Kempf and T. Yamada of Abbott Laboratories, S. Ichinose of Instrumental Analysis Research Center and S. Endo of Animal Research Center, Tokyo Medical and Dental University for their advice and assistance with the experiments. We also thank Y. Sato of the National Institute of Infectious Diseases for her excellent technical assistance.

References

1. Rickinson AB, Kieff E. Epstein-Barr virus. In: Fields BN, ed. Fields virology, 4th edn. New York (NY): Lippincott Williams and Wilkins, 2001. Vol. 1, 2575–627.
2. Kieff E, Rickinson AB. Epstein-Barr virus and replication. In: Fields BN, ed. Fields virology, 4th ed. New York (NY): Lippincott Williams and Wilkins, 2001. Vol. 1, 2511–73.
3. Zur Hausen H, Schulte-Holthausen H. Presence of EB virus nucleic acid homology in a "virus-free" line of Burkitt tumour cells. Nature 1970;227:245–48.
4. Nonoyama M, Pagano JS. Homology between Epstein-Barr virus DNA and viral DNA from Burkitt's lymphoma and nasopharyngeal carcinoma determined by DNA-DNA reassociation kinetics. Nature 1973;242:44–7.
5. Rowe M, Lear AL, Croom-Carter D, Davies AH, Rickinson AB. Three pathways of Epstein-Barr virus gene activation from EBNA1-positive latency in B lymphocytes. J Virol 1992;66:122–31.
6. Yamamoto N, Takizawa T, Iwanaga Y, Shimizu N, Yamamoto N. Malignant transformation of B lymphoma cell line BJAB by Epstein-Barr virus-encoded small RNAs. FEBS Lett 2000;484:153–58.
7. Mosialos G, Birkenbach M, Yalamanchili R, VanArsdale T, Ware C, Kieff E. The Epstein-Barr virus transforming protein LMP1 engages signaling proteins for the tumor necrosis factor receptor family. Cell 1995;80:389–99.
8. Mori N, Fujii M, Ikeda S, Yamada Y, Tomonaga M, Ballard DW, Yamamoto N. Constitutive activation of NF-κB in primary adult T-cell leukemia cells. Blood 1999;93:2360–8.
9. Baldwin AS. The NF-κB and IκB proteins: new discoveries and insights. Annu Rev Immunol 1999;14:649–81.
10. Guinness ME, Kenney JL, Reiss M, Lacy J. Bcl-2 antisense oligodeoxynucleotide therapy of Epstein-Barr virus-associated lymphoproliferative disease in severe combined immunodeficient mice. Cancer Res 2000;60:5354–8.
11. Miyake A, Dewan MZ, Ishida T, Watanabe M, Honda M, Sata T, Yamamoto N, Umezawa K, Watanabe T, Horie R. Induction of apoptosis in Epstein-Barr virus-infected B-lymphocytes by the NF-kappaB inhibitor DHMEQ. Microbes Infect 2008;10:748–56.
12. Watanabe M, Dewan MZ, Okamura T, Sasaki M, Itoh K, Higashihara M, Mizoguchi H, Honda M, Sata T, Watanabe T, Yamamoto N, Umezawa K, et al. A novel NF-κB inhibitor DHMEQ selectively targets constitutive NF-κB activity and induces apoptosis of multiple myeloma cells in vitro and in vivo. Int J Cancer 2005;114:32–8.
13. Adams J, Palombella VJ, Elliott PJ. Proteasome inhibition: a new strategy in cancer treatment. Invest New Drugs 2001;18:109–21.
14. Teicher BA, Ara G, Herbst R, Palombella VJ, Adams J. The proteasome inhibitor PS-341 in cancer therapy. Clin Cancer Res 1999; 5:2638–45.

15. Hideshima T, Chauhan D, Richardson P, Mitsiades C, Mitsiades N, Hayashi T, Munshi N, Dang L, Castro A, Palombella V, Adams J, Anderson KC. NF-κB as a therapeutic target in multiple myeloma. J Biol Chem 2002;277:16639–47.
16. Dewan MZ, Terashima K, Taruishi M, Hasegawa H, Ito M, Tanaka Y, Mori N, Sata T, Koyanagi Y, Maeda M, Kubuki Y, Okayama A, et al. Rapid tumor formation of human T-cell leukemia virus type 1-infected cell lines in novel NOD-SCID/γc^{null} mice: suppression by an inhibitor against NF-κB. J Virol 2003;77:5286–94.
17. Kitajima I, Shinohara T, Bilakovics J, Brown DA, Xu X, Nerenberg M. Ablation of transplanted HTLV-1 Tax-transformed tumors in mice by antisense inhibition of NF-κB. Science 1992;258:1792–5.
18. Mori N, Yamada Y, Ikeda S, Yamasaki Y, Tsukasaki K, Tanaka Y, Tomonaga M, Yamamoto N, Fujii M. Bay 11–7082 inhibits transcription factor NF-κB and induces apoptosis of HTLV-I-infected T-cell lines and primary adult T-cell leukemia cells. Blood 2002;100:1828–34.
19. Tan C, Waldmann TA. Proteasome inhibitor PS-341, a potential therapeutic agent for adult T-cell leukemia. Cancer Res 2002;62: 1083–6.
20. Dewan MZ, Uchihara JN, Terashima K, Honda M, Sata T, Ito M, Fujii N, Uozumi K, Tsukasaki K, Tomonaga M, Kubuki Y, Okayama A, et al. Efficient intervention of growth and infiltration of primary adult T-cell leukemia cells by an HIV protease inhibitor, ritonavir. Blood 2006;107:716–24.
21. Cahir-McFarland ED, Davidso DM, Schauer SL, Duong J, Kieff E. NF-kappa B inhibition causes spontaneous apoptosis in Epstein-Barr virus-transformed lymphoblastoid cells. Proc Natl Acad Sci USA 2000;97:6055–60.
22. Collier AC. Efficacy of combination antiretroviral therapy. Adv Exp Med Biol 1996;394:355–72.
23. Collier AC, Coombs RW, Schoenfeld DA, Bassett R, Baruch A, Corey L. Combination therapy with zidovudine, didanosine and saquinavir. Antiviral Res 1996;29:99.
24. Collier AC, Coombs RW, Schoenfeld DA, Bassett RL, Timpone J, Baruch A, Jones M, Facey K, Whitacre C, McAuliffe VJ, Friedman HM, Merigan TC, et al. Treatment of human immunodeficiency virus infection with saquinavir, zidovudine, and zalcitabine. AIDS Clinical Trials Group. N Engl J Med 1996;334:1011–17.
25. Markowitz M, Saag M, Powderly WG, Hurley AM, Hsu A, Valdes JM, Henry D, Sattler F, La Marca A, Leonard JM, Ho DD. A preliminary study of ritonavir, an inhibitor of HIV-1 protease, to treat HIV-1 infection. N Engl J Med 1995;333:1534–39.
26. Kempf DJ, Marsh KC, Denissen JF, McDonald E, Vasavanonda S, Flentge CA, Green BE, Fino L, Park CH, Kong XP, Wideburg NE, Saldivar A, et al. ABT-538 is a potent inhibitor of human immunodeficiency virus protease and has high oral bioavailability in humans. Proc Natl Acad Sci USA 1995;92:2484–88.
27. Andre P, Groettrup M, Klenerman P, de Giuli R, Booth BL, Jr, Cerundolo V, Bonneville M, Jotereau F, Zinkernagel RM, Lotteau V. An inhibitor of HIV-1 protease modulates proteasome activity, antigen presentation, and T cell responses. Proc Natl Acad Sci USA 1998; 95:13120–24.
28. Liang JS, Distler O, Cooper DA, Jamil H, Deckelbaum RJ, Ginsberg HN, Sturley SL. HIV protease inhibitors protect apolipoprotein B from degradation by the proteasome: a potential mechanism for protease inhibitor-induced hyperlipidemia. Nat Med 2001;7:1327–31.
29. Schmidtke G, Holzhütter HG, Bogyo M, Kairies N, Groll M, de Giuli R, Emch S, Groettrup M. How an inhibitor of the HIV-I protease modulates proteasome activity. J Biol Chem 1999;274:35734–40.
30. Gaedicke S, Firat-Geier E, Constantiniu O, Lucchiari-Hartz M, Freudenberg M, Galanos C, Niedermann G. Antitumor effect of the human immunodeficiency virus protease inhibitor ritonavir: induction of tumor-cell apoptosis associated with perturbation of proteasomal proteolysis. Cancer Res 2002;62:6901–8.
31. Pati S, Pelser CB, Dufraine J, Bryant JL, Reitz JMS, Weichold FF. Antitumorigenic effects of HIV protease inhibitor ritonavir: inhibition of Kaposi sarcoma. Blood 2002;99:3771–9.
32. Sgadari C, Barillari G, Toschi E, Carlei D, Bacigalupo I, Baccarini S, Palladino C, Leone P, Bugarini R, Malavasi L, Cafaro A, Falchi M, et al. HIV protease inhibitors are potent anti-angiogenic molecules and promote regression of Kaposi sarcoma. Nat Med 2002;8:225–32.
33. Katano H, Pesnicak H, Cohen JI. Simvastatin induces apoptosis of Epstein-Barr virus (EBV)-transformed lymphoblastoid cell lines and delays development of EBV lymphomas. Proc Natl Acad Sci USA 2004;101:4960–5.
34. Norvir, Ritonavir Product monograph. North Chicago, IL: Abbott laboratories, 1997.
35. Gatti G, Di Biagio A, Casazza R, De Pascalis C, Bassetti M, Cruciani M, Vella S, Bassetti D. The relationship between ritonavir plasma levels and side-effects: implications for therapeutic drug monitoring. AIDS 1999;13:2083–9.

THE JOURNAL OF BIOLOGICAL CHEMISTRY VOL. 284, NO. 36, pp. 23980–23988, September 4, 2009

Pin1 Catalyzes Conformational Changes of Thr-187 in p27^{Kip1} and Mediates Its Stability through a Polyubiquitination Process*[S]

Received for publication, May 19, 2009, and in revised form, July 3, 2009 Published, JBC Papers in Press, July 7, 2009, DOI 10.1074/jbc.M109.022814

Wei Zhou[‡], Qiaoyun Yang[‡], Choon Bing Low[‡], Balakrishna Chandrababu Karthik[‡], Yu Wang[‡], Akihide Ryo[§], Shao Q. Yao[‡¶], Daiwen Yang[‡], and Yih-Cherng Liou[‡1]

From the Departments of [‡]Biological Sciences and [¶]Chemistry, National University of Singapore, 14 Science Drive 4, Singapore 117543, Singapore and the [§]1st Research Group, AIDS Research Center, National Institute of Infectious Disease (1), 4-7-1 Gagkuen, Musashimurayama, Tokyo 208-0011, Japan

The *cis-trans* peptidylprolyl isomerase Pin1 plays a critical role in regulating a subset of phosphoproteins by catalyzing conformational changes on the phosphorylated Ser/Thr-Pro motifs. The phosphorylation-directed ubiquitination is one of the major mechanisms to regulate the abundance of p27^{Kip1}. In this study, we demonstrate that Pin1 catalyzes the *cis-trans* conformational changes of p27^{Kip1} and further mediates its stability through the polyubiquitination mechanism. Our results show that the phosphorylated Thr-187-Pro motif in p27^{Kip1} is a key Pin1-binding site. In addition, NMR analyses show that this phosphorylated Thr-187-Pro site undergoes conformational change catalyzed by Pin1. Moreover, in Pin1 knock-out mouse embryonic fibroblasts, p27^{Kip1} has a shorter lifetime and displays a higher degree of polyubiquitination than in Pin1 wild-type mouse embryonic fibroblasts, suggesting that Pin1 plays a critical role in regulating p27^{Kip1} degradation. Additionally, Pin1 dramatically reduces the interaction between p27^{Kip1} and Cks1, possibly via isomerizing the *cis-trans* conformation of p27^{Kip1}. Our study thus reveals a novel regulatory mechanism for p27^{Kip1} stability and sheds new light on the biological function of Pin1 as a general regulator of protein stability.

Cellular differentiation and cell cycle inhibition are tightly controlled via sensitive molecular mechanisms. p27^{Kip1}, a member of the Cip/Kip family, is an essential cell cycle inhibitor that functions largely during the G_0/G_1 phase where it promotes the assembly of the cyclin D1-CDK4 complex and inhibits the kinase activity of the cyclin E-CDK2 complex in the G_1-S phase (1–4). Several review articles have elegantly summarized and discussed the detailed cellular functions of p27^{Kip1} (1–6). p27^{Kip1} is also a phosphoprotein with multiple Ser/Thr phosphorylation sites, including Ser-10, Ser-178, and Thr-187, followed by a proline residue. Hence, these motifs are potential substrate sites for proline-directed kinases (5, 6). Compared with Ser-178, which has not yet been well studied, the phosphorylation of Ser-10 and Thr-187 has been well characterized to be important for the regulation of p27^{Kip1} function. For instance, Ser-10 has been found to be the major phosphorylation site of p27^{Kip1} (7) and to play an important role in regulating cell migration (8–10), although the regulation of Ser-10 phosphorylation is still not completely defined (11, 12).

In contrast to Ser-10 and Thr-178, Thr-187 is the best characterized phosphorylation site on p27^{Kip1} and is known to regulate the complex formation of p27^{Kip1}-cyclin E-CDK2 (1–2). In addition, it is also widely accepted that Thr-187 plays a crucial role in determining the abundance of mature p27^{Kip1} proteins. The phosphorylation of Thr-187 directs p27^{Kip1} to an SCF^{Skp2} ubiquitin ligase complex (consisting of Skp2-Skp1-Cks1-Cul1-Roc1), which in turn promotes the polyubiquitination and degradation of p27^{Kip1} (13, 14). The crystal structure of the Skp1-Skp2-Cks1-p27^{Kip1} phosphopeptide complex shows that p27^{Kip1} binds both Cks1 and Skp2 and that the C terminus of Skp2 and Cks1 forms the substrate recognition core of the SCF complex (15). Furthermore, the structure of this complex has revealed that the phosphorylation of Thr-187 in p27^{Kip1} is recognized by the phosphate-binding site of Cks1, indicating that Cks1 is not only a facilitator but also an indispensable component in p27^{Kip1} degradation machinery (15).

Pin1 is a unique peptidyl-prolyl isomerase (PPIase)[2] that recognizes only the phosphorylated Ser/Thr motif preceding a proline residue (16). In addition, Pin1 is very prominent in isomerizing the *cis-trans* conformation of prolyl-peptidyl bonds in its substrates, resulting in either the modification of their function (*e.g.* c-Jun (17), β-catenin (18), Bax (19), and Notch1 (20)) or modulation of their stability (*e.g.* cyclin D1 (21), p53 (22, 23), and NF-κB (24)). Loss of Pin1 in mice results in several phenotypes similar to those of cyclin D1-null mice (21) and neuronal degenerative phenotypes (25–28), suggesting the conformational changes mediated by Pin1 may be crucial for the normal functioning of cells. Additionally, Pin1 also plays important roles in cancer and other cellular events, which have

* This work was supported by Grant 06/1/21/19/473 from the Biomedical Research Council, the Agency for Science, Research, and Technology, and in part by Facility Research Council Grant R-154-000-403-112 from the National University of Singapore (to Y. C. L.).

[S] The on-line version of this article (available at http://www.jbc.org) contains supplemental Experimental Procedures, Results, and Figs. S1–S3.

[1] To whom correspondence should be addressed: 14 Science Dr. 4, Singapore 117543, Singapore. Tel.: 65-6516-7711; Fax: 65-6779-2486; E-mail: dbslyc@nus.edu.sg.

[2] The abbreviations used are: PPIase, peptidylprolyl isomerase; MEF, mice embryonic fibroblast; CIP, calf intestinal phosphatase; WT, wild type; GST, glutathione *S*-transferase; HEK, human embryonic kidney; ROESY, rotating frame Overhauser effect spectroscopy; SCF, SKP1-CUL1-F-box; pRb, retinoblastoma protein.

been extensively discussed in several recent review articles (29–33).

In this study, we show that Pin1 binds to p27^{Kip1}, mainly through the phosphorylated Thr-187-Pro motif, and causes subsequent prolyl isomerization of this cell cycle protein. Moreover, we also find that Pin1 can protect p27^{Kip1} from degradation. Importantly, we demonstrate that by catalyzing conformational changes in p27^{Kip1}, Pin1 hinders its association with Cks1, resulting in a reduction of polyubiquitination of p27^{Kip1} and protecting its degradation by SCF^{Skp2} complexes. Our results suggest that the *cis-trans* isomerization catalyzed by Pin1 represents a novel regulatory mechanism during post-phosphorylation of proteins and polyubiquitination-directed degradation pathways.

EXPERIMENTAL PROCEDURES

Constructs, Reagents, and Antibodies—Full-length cDNAs for p27^{Kip1}, Cks1, and Skp2 were cloned from a HeLa cDNA library and inserted into the pXJ-40-FLAG vector and/or pXJ-40-GFP vector (a gift from Dr. B. C. Low, Department of Biological Sciences, National University of Singapore) or into p3x-FLAG-CMV vector (Sigma). Recombinant proteins of the full-length human Pin1, and its WW and PPIase domains, were expressed from the pET42b(+) vector (Novagen). All mutant constructs were generated using the QuikChange® site-directed mutagenesis kit (Stratagene). Cycloheximide, FLAG-M2 beads, and MG132 were purchased from Sigma. Okadaic acid was purchased from Santa Cruz Biotechnology. Antibodies used for Western blotting and pulldown assays were as follows: polyclonal antibody against p27^{Kip1} (C-19), monoclonal antibody against p27^{Kip1} (F-8), polyclonal antibodies against Ser(P)-10-p27^{Kip1}, Skp2 (H-435), Cks1 (FL-79), and ubiquitin (P4D1) (Santa Cruz Biotechnology); polyclonal antibody against Thr(P)-187-p27^{Kip1} (Zymed Laboratories Inc.); monoclonal antibodies against α-tubulin and FLAG (Sigma).

Cell Culture and Transfection—Human embryonic kidney (HEK) epithelial 293T cells and Pin1-WT (wild-type) and Pin1-KO (knock-out) mouse embryonic fibroblasts (MEFs; a gift from Dr. K. P. Lu, Department of Medicine, Beth Israel Deaconess Medical Center, Harvard Medical School) were maintained in Dulbecco's modified Eagle's medium supplemented with 10% fetal bovine serum, 1% penicillin/streptomycin unless otherwise noted. For overexpression analysis, all constructs into MEFs were transfected using Lipofectamine (Invitrogen) according to the manufacturer's protocol. HEK 293T cells were transfected using the calcium phosphate method. Following transfection, cells were harvested in mammalian lysis buffer (50 mM Tris-HCl, pH 7.4, 100 mM NaCl, 10% glycerol, 1% Triton X-100, 1 mM EDTA, supplemented with protease inhibitors and phosphatase inhibitors, including 1 μM pepstatin, 1 μM leupeptin, 50 μM β-glycerophosphatase, 1 mM okadaic acid, 1 mM Na_3VO_4).

GST Pulldown and Co-immunoprecipitation Assays—For GST pulldown assay, recombinant GST-full-length Pin1, -WW, or -PPIase domain proteins were conjugated to glutathione-Sepharose 4B beads. Beads were rocked with lysates from cells overexpressing WT or mutant p27^{Kip1} constructs for 3 h at 4 °C, followed by five washes with mammalian lysis buffer. The bound proteins were eluted with SDS-loading dye and resolved by 12–15% SDS-PAGE, followed by Western blotting. Calf intestinal phosphatase (CIP) treatments were performed as described previously (23). CIP, 1 unit/ml (Promega), was added to the cell lysates for 30 min at 30 °C, which were then subjected to GST pulldown. For co-immunoprecipitation, FLAG-p27^{Kip1} and mutant constructs were overexpressed in HEK 293T cells. Cell lysates were then cleared by centrifugation at 13,000 rpm for 10 min, and the resulting supernatants were incubated with FLAG-M2 beads for 3–5 h at 4 °C. The bound proteins were then analyzed by Western blotting.

Protein Stability Assay—Pin1-WT and -KO MEF cells were transfected with FLAG-p27^{Kip1} WT or mutant constructs. Within 24 h of transfection, cycloheximide (100 μg/ml) was added to the cells to block protein synthesis. Cells were then harvested at 4-h intervals, followed by Western blotting.

In Vivo Ubiquitination Assay—FLAG-p27^{Kip1} and Myc-ubiquitin constructs were co-transfected into Pin1-WT and -KO MEF cells, respectively. At 24 h following transfection, cells were treated with 10 μM MG132 to inhibit protein degradation. After 3 h of drug treatment, cells were harvested. The supernatants of cell lysates were then incubated with FLAG-M2 beads at 4 °C for 3 h, followed by five washes with mammalian lysis buffer and Western blotting using anti-ubiquitin antibody. The membranes were subsequently stripped and re-blotted with anti-p27^{Kip1} antibody to evaluate the amount of p27^{Kip1} that had bound to the beads. Reciprocal experiments were carried out by co-overexpressing FLAG-ubiquitin and GFP-p27^{Kip1} in Pin1-WT and KO MEF cells. After MG312 treatment, cell lysates were subjected to pulldown assays using FLAG-M2 beads. Consequently, the beads were cooked at 95 °C for 5 min. Western blotting analyses were done using either anti-p27^{Kip1} or anti-ubiquitin antibody.

Conformational Change by NMR Spectroscopy—All NMR experiments were performed using a Bruker 800-MHz NMR spectrometer at 25 °C. All spectra were recorded for a 2.0 mM peptide concentration dissolved in a 20 mM phosphate buffer (90% H_2O and 10% D_2O, pH 6.5) in the presence or absence of 0.03 mM Pin1. For all experiments, 256 × 512 complex points were acquired with spectral widths of 7200 × 9600 Hz in $t_1 \times t_2$ dimensions and a relaxation delay of 1 s. ROESY spectra (34) were acquired at a mixing time of 110 ms, a spin-lock field strength of 4 kHz, and 16 scans. The mixing times were 30, 50, 70, 90, and 110 ms. TOSCY experiments (35) were carried out at a mixing time of 75 ms and 8 scans.

RESULTS

Interaction of Pin1 and Phosphorylated p27^{Kip1}—Observations from our several preliminary experiments led us to speculate that Pin1 may associate with p27^{Kip1} (supplemental Fig. S1). Sequence analysis also showed that p27^{Kip1} contains three potential Pin1-binding Ser/Thr-Pro motifs as follows: S10P, S178P, and T187P (Fig. 1*A*). To confirm that Pin1 could interact with p27^{Kip1}, we performed glutathione *S*-transferase (GST) pulldown assays using recombinant GST-Pin1, GST-Pin1-W34A (impaired WW domain-binding site), and GST-Pin1-R68A/R69A mutants (impaired PPIase domain-binding sites) or GST proteins to pull down FLAG-p27^{Kip1} protein overex-

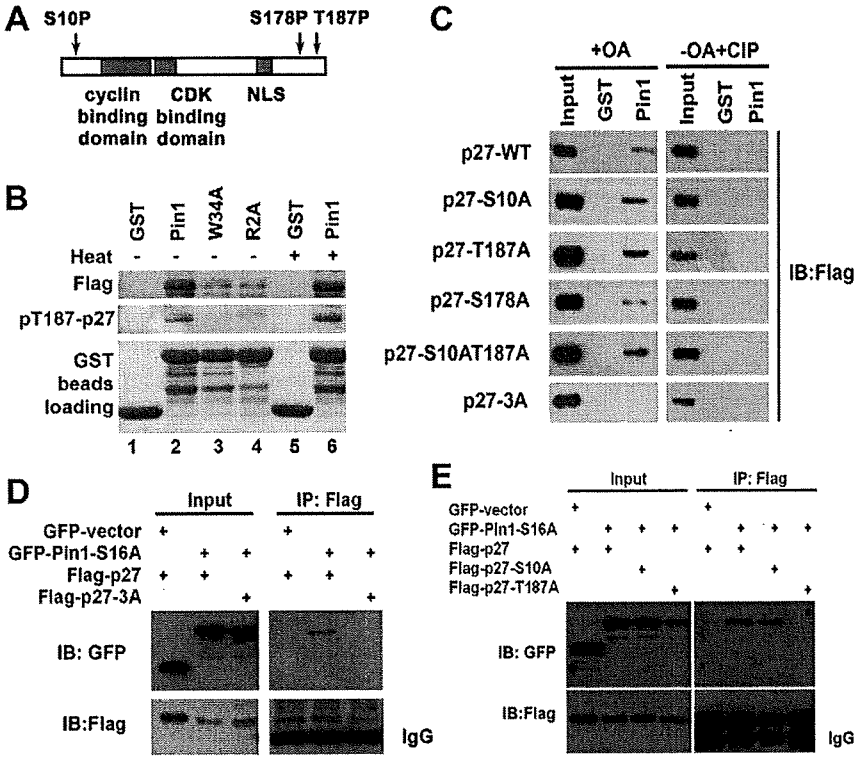

FIGURE 1. **Pin1 binds the Ser/Thr-Pro motifs of p27^{Kip1} through its WW and PPIase domain.** *A*, schematic illustration of the potential Pin1-binding sites in p27^{Kip1}, which includes the S10P (Ser-10-Pro), S178P (Ser-178-Pro), and T187P (Thr-187-Pro) motifs. *NLS*, nuclear localization signal. *B*, immunoblotting analysis following the use of GST-Pin1, GST-Pin1-W34A (W34A mutant), and GST-Pin1-R2A (R68A/R69A mutants) to pull down FLAG-p27^{Kip1}. GST beads were used as a control. GST and GST-Pin1 proteins were stained as loading controls. *C*, immunoblotting (*IB*) analyses following the use of GST-Pin1 or GST beads to pull down either FLAG-p27^{Kip1} or -p27^{Kip1} mutants, in the absence (*left panel*) or presence (*right panel*) of CIP. *OA*, okadaic acid; *CIP*, calf intestinal phosphatase. *D*, co-immunoprecipitation (*IP*) assay using FLAG-M2 beads. GFP-Pin1-S16A was co-immunoprecipitated with FLAG-p27^{Kip1}, but not a FLAG-p27^{Kip1}-3A mutant. *E*, GFP-Pin1-S16A was co-immunoprecipitated with either the FLAG-p27^{Kip1}-WT or the FLAG-p27^{Kip1}-S10A mutant but not with the FLAG-p27^{Kip1}-T187A mutant.

pressed in HEK 293T cells. As shown in Fig. 1*B*, our results indicate that GST-Pin1 interacts with FLAG-p27^{Kip1}, but not GST control, indicating that Pin1 can bind p27^{Kip1} *in vitro* (Fig. 1*B*, *1st* and *2nd lanes*). It is also known that both WW and PPIase domains of Pin1 can bind phosphorylated Ser/Thr-Pro motifs (36). Therefore, we further performed GST pulldowns using Pin1-W34A and Pin1-R68A/R69A mutants to identify the region of Pin1 that is responsible for p27^{Kip1} binding. Notably, neither GST-Pin1-W34A nor GST-Pin1-R68A/R69A mutant associates strongly with p27^{Kip1} protein compared with GST-Pin1-WT, suggesting that both the WW and PPIase domains are required for an efficient Pin1-p27^{Kip1} interaction (Fig. 1*B*, *3rd* and *4th lanes*). To further test for a direct interaction of p27^{Kip1} with Pin1, which does not rely on any bridging proteins, cell lysates with overexpressed FLAG-p27^{Kip1} were subjected to heating at 95 °C for 10 min before GST pulldown because p27^{Kip1} is an intrinsically heat-stable protein (13). As shown in Fig. 1*B* (*5th* and *6th lanes*), the Pin1-p27^{Kip1} interaction is intact after the heat treatment, indicating that p27^{Kip1} directly interacts with Pin1 *in vitro*. In addition, using an antibody specifically against phosphorylated p27^{Kip1}, we also found that Pin1 interacts with phosphorylated p27^{Kip1} (Fig. 1*B*).

To identify the preferred Pin1-binding motif in p27^{Kip1}, we constructed a series of p27^{Kip1} mutants by substituting Ser/Thr for Ala at its three putative Pin1-binding sites. We then performed GST pulldown and co-immunoprecipitation assays. Fig. 1*C* shows that Pin1 binds WT, all single mutants, and one double mutant of p27^{Kip1}. However, the triple mutation (3A) of p27^{Kip1} totally abolishes this association (Fig. 1*C*, *left panel*), indicating that Ser-10, Ser-178, and Thr-187 of p27^{Kip1} may all be involved in Pin1-p27^{Kip1} binding *in vitro*. Given that Pin1 only binds phosphoproteins, and to confirm that the binding of Pin1 to p27^{Kip1} is phosphorylation-dependent, we incubated cell lysates with CIP before performing GST pulldown assays. As shown in Fig. 1*C* (*right panel*), the interactions between Pin1 and p27^{Kip1} WT/mutants are completely disrupted by CIP treatment, suggesting that the binding of Pin1 to p27^{Kip1} is phosphorylation-dependent. By next co-overexpressing FLAG-p27^{Kip1} and GFP-Pin1-S16A, a stronger binding derivative of Pin1 (37), the co-immunoprecipitation assays further demonstrated that Pin1 binds p27^{Kip1} WT but not the triple mutant (3A) *in vivo* (Fig. 1*D*), consistent with the GST pulldown results (Fig. 1*C*). Interestingly, we observed that the p27^{Kip1} S10A mutant co-immunoprecipitated significantly with Pin1 (Fig. 1*E*) but that there was almost no interaction between Pin1 and the p27^{Kip1} T187A mutant. Taken together, these results suggest that Thr-187 could be the major Pin1-binding site in p27^{Kip1} *in vivo* (Fig. 1*E*).

A single Ala residue substitution at the Ser/Thr-Pro motifs of p27^{Kip1} did not totally eliminate the interaction between Pin1 and p27^{Kip1} in GST pulldown assays (Fig. 1*C*). Hence, to further elucidate the binding property of the Pin1-p27^{Kip1} interaction, we developed phosphopeptide chips for binding analysis. To this end, three N-terminal biotinylated phosphopeptides derived from Ser/Thr-Pro motifs in p27^{Kip1} were synthesized (Fig. 2*B*). Subsequently, we immobilized these three biotinylated-p27^{Kip1} peptides on glass slides coated with avidin to generate peptide chips, as described previously (38, 39). To determine the affinity of Pin1 to these peptides, different concentrations of Cy3-labeled Pin1 were titrated on chips. The fluorescence reading for each spot was then extracted from the unbound background intensities and fitted to binding curves for individual Pin1-peptide interaction (Fig. 2*A*). A smaller K_d value indicates a stronger binding. As shown in Fig. 2*B*, Pin1 binds most strongly to the phosphorylated Thr-187 peptide,

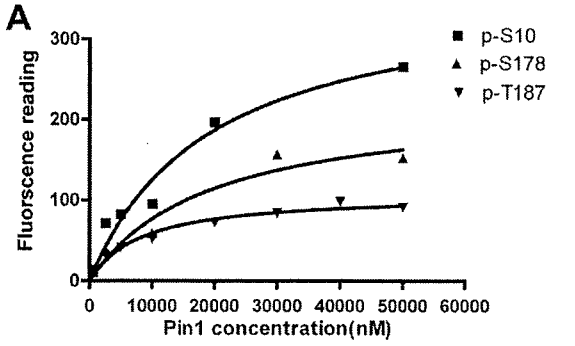

B

Name	Sequence	Kd(μM)	SD(μM)
p-S10	VRVSNG**pS**PSLERMD	16.0	4.7
p-S178	ENVSDG**pS**PNAGSVE	15.7	5.2
p-T187	AGSVEG**pT**PKKPGLR	7.2	1.5

FIGURE 2. **Phosphorylated Thr-187 is the major Pin1-binding site on p27^{Kip1}.** *A*, fitted binding curves for Pin1 recombinant protein bound to three phosphorylated peptides derived from p27^{Kip1}. *B*, phosphorylated peptide sequences and K_d and S.D. values calculated from the binding curve shown in *A*, indicating the affinity of Pin1 for phosphorylated peptides derived from p27^{Kip1}.

with a dissociation constant (K_d) of ~7.2 μM. In contrast, Pin1 has a weaker affinity for phosphorylated Ser-10 or Ser-178 peptides with K_d values of ~16 μM. Therefore, taken together both *in vitro* and *in vivo* binding assays confirm that the phosphorylated Thr-187 residue on p27^{Kip1} is the major Pin1-binding site.

Pin1 Accelerates Conformational Changes in p27^{Kip1}—Pin1 is a peptidylprolyl isomerase and accelerates conformational changes between the *cis* and *trans* forms of phosphorylated polypeptides. In addition to its binding of cognate substrates, the best way to demonstrate the function of Pin1 is to measure these catalytically driven conformational changes. To this end, we analyzed the isomerase activity of Pin1 against nonphosphorylated (Fig. 3*A*) and phosphorylated Thr-187-Pro peptides (GSVEG**pT**PKKPGA, where boldface indicates positions 6 and 8, respectively), in the absence of (Fig. 3B) or presence of Pin1 (Fig. 3C). Because of the slow exchange between *cis* and *trans* conformations of proline, several residues in both peptides displayed two distinct sets of ^{1}H signals in the ROESY and total correlation spectroscopy spectra (Fig. 3, *B* and *C*). The *cis* and *trans* populations of both peptides were ~10 and 90%, respectively, as estimated from the one-dimensional ^{1}H spectrum. In a normal situation, the exchange between the *cis* and *trans* conformations was so slow on an NMR time scale; therefore, no cross-peaks between the two conformations were observed by NMR (<0.1 s^{-1}, see Fig. 3*B*). In contrast, in the presence of Pin1, the proline isomerization rate of the phosphorylated peptide is greatly enhanced by Pin1. Cross-peaks from conformational exchange were also identified (Fig. 3*B*). Both cross-peaks and diagonal peaks of Thr-6 and Lys-8 amide protons from the phosphorylated Thr-187 peptides were also found (Fig. 3*B*). On the other hand, the nonphosphorylated peptide displayed no exchange peaks, even in the presence of Pin1 (Fig. 3*A*). Hence, Pin1 only accelerates the isomerization of the phosphorylated Thr-187 peptide in p27^{Kip1} (Fig. 3*C*) but not the nonphosphorylated control (Fig. 3*A*).

Taking the intensities of cross-peaks and diagonal peaks of Thr-6 and Lys-8 amide protons of phosphopeptide, we further calculated the isomerization rates from the *cis* to *trans* (k_{ct}^{cat}) and from the *trans* to *cis* (k_{tc}^{cat}) conformations of Thr-6 (Fig. 3, *D* and *E*). The values of k_{ct}^{cat}- and k_{tc}^{cat}-obtained intensities for Thr-6 were 1.08 and 0.12 s^{-1}, respectively. Similarly, the values of k_{ct}^{cat}- and k_{tc}^{cat}-obtained intensities for Thr-8 were 1.05 and 0.15 s^{-1}, respectively (data not shown). The enhanced *cis-trans* conformational exchange rate by more than 10-fold suggests that the isomerization rates catalyzed by Pin1 are significantly faster than those without Pin1 (Fig. 3*F*).

Pin1 Protects p27^{Kip1} from Degradation—Phosphorylation on Thr-187 was known to be very important for p27^{Kip1} degradation (6, 40). Our current results show that Pin1 catalyzes p27^{Kip1} through its phosphorylated Thr-187-Pro motif (Fig. 3). We next speculated whether Pin1 is involved in regulating p27^{Kip1} stability. To test this possibility, we measured endogenous p27^{Kip1} levels and found them to be dramatically lower, by about 50%, in Pin1-KO MEFs compared with Pin1-WT MEFs (Fig. 4, *A* and *B*); as previously reported, in our Pin1-KO MEFs, the cyclin D1 levels are markedly decreased (21), and cyclin E is significantly increased (41) (Fig. 4*A*). Consistently, we also find in our present experiments that a knockdown of Pin1 using small interfering RNA causes a decrease of the p27^{Kip1} levels in HEK 293T cells (supplemental Fig. S2). This observation indicates that Pin1 is able to stabilize p27^{Kip1} protein. Subsequently, we compared the half-life of endogenous p27^{Kip1} in both Pin1-WT and -KO MEFs exposed to cycloheximide. As shown in Fig. 4*C*, the endogenous p27^{Kip1} levels in Pin1-KO MEFs are significantly less stable than those in Pin1-WT MEFs. After 12 h of cycloheximide inhibition, endogenous p27^{Kip1} is markedly reduced by up to ~76% in the absence of Pin1. In contrast, only a 50% reduction of p27^{Kip1} is evident in Pin1-WT MEFs (Fig. 4, *C* and *D*). To demonstrate that the destabilization of p27^{Kip1} is a direct effect of the absence of Pin1, we investigated the turnover rate of p27^{Kip1} by re-introducing GFP-Pin1 into Pin1-KO MEFs. As shown in Fig. 4, *C* and *D*, the stability of p27^{Kip1} is markedly enhanced by re-overexpression of GFP-Pin1, but not GFP alone, in Pin1-KO MEFs, suggesting that Pin1 plays a critical role in modulating p27^{Kip1} stability.

To clearly determine whether Pin1 specifically regulates p27^{Kip1} stability through the phosphorylated Thr-187 site, we investigated this stability in the presence or absence of Pin1 using the p27^{Kip1} double mutants, S10A/S178A (potential Thr(P)-187), S10A/T187A (potential Ser(P)-178), and S178A/T187A (potential Ser(P)-10), instead of single mutants of p27^{Kip1}. We found that the stability of the two mutants containing T187A and the triple mutant (3A) showed no significant difference in the presence or absence of Pin1 (Fig. 4*E*). Furthermore, even though Pin1 may potentially interact with Ser(P)-10 (Fig. 1), the S178A/T187A mutant (potential Ser(P)-10) has no significant difference in turnover rate between Pin1-WT (73% remaining) and -KO MEFs (76% remaining), suggesting that Pin1 has little or no effect on p27^{Kip1} degradation through the Ser-10 site. Most importantly, the double mutant S10A/S178A (potential Thr(P)-187) displays a shorter half-life in the absence of Pin1, degrading 66% of its total level (Fig. 4*E*), underscoring the significance of Thr-187 of p27^{Kip1} for Pin1 function.

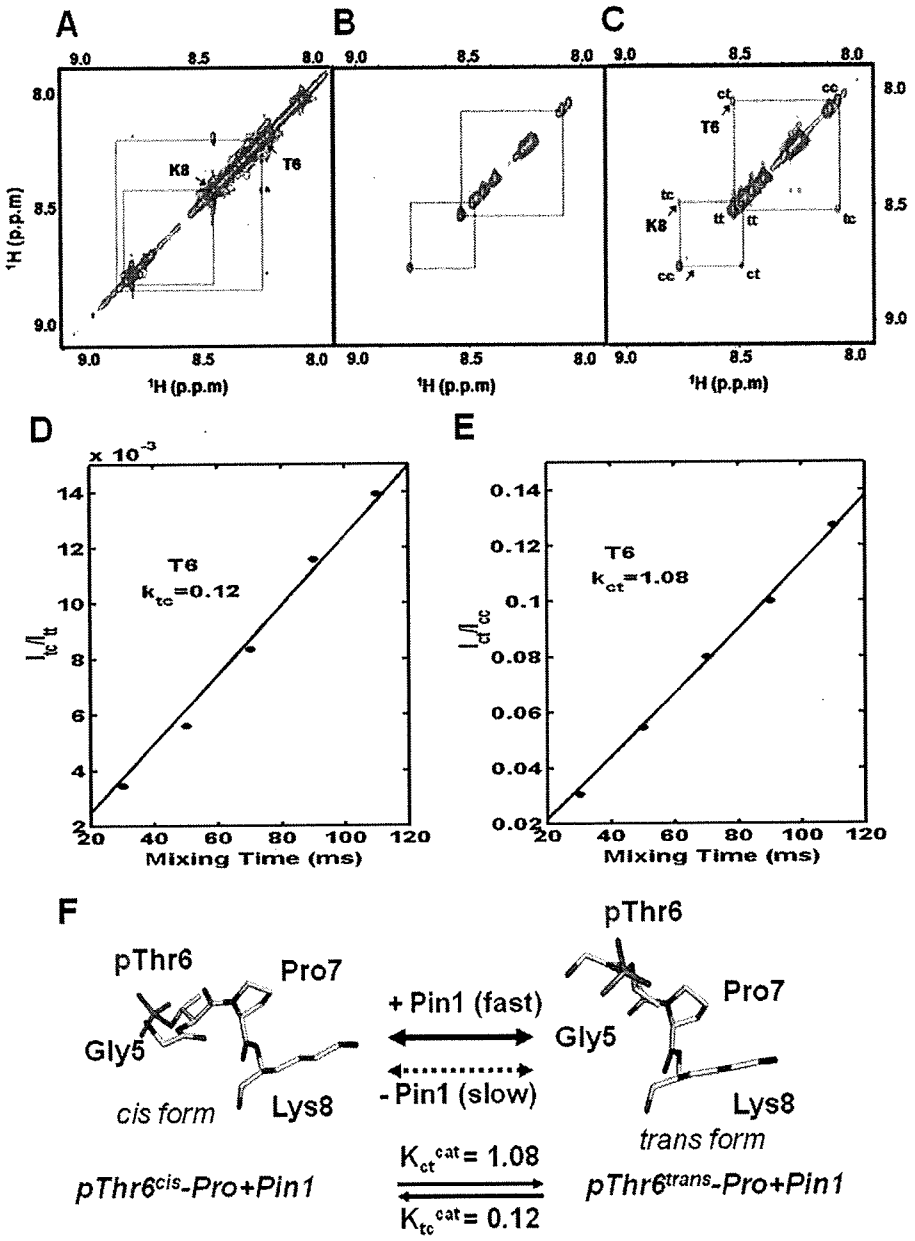

FIGURE 3. **Pin1 catalyzes conformational changes in phosphorylated p27^{Kip1}.** *A*, selected region of a two-dimensional ROESY spectrum of a nonphosphorylated Thr-187 peptide (AGSVEGTPKKPGLR) at a concentration of 2.4 mM and in the presence of 0.03 mM Pin1 (mixing time 110 ms) is shown. There is no cross-peak found (as indicated by *arrows*). *B* and *C*, selected regions of a two-dimensional ROESY spectrum of a phosphorylated Thr-187 peptide (GSVEG**pT**P**K**KPGA, where boldface indicates positions 6 and 8, respectively) at a concentration of 2.0 mM are shown in the absence (*B*) or in the presence (*C*) of 0.03 mM Pin1 (mixing time 110 ms). Negative and positive peaks are indicated by *arrows*. Diagonal peaks from *cis* and *trans* conformers are indicated by *cc* and *tt*, respectively. Exchange peaks resulting from Pin1-catalyzed isomerization are labeled *ct* and *tc*. Note that rotating frame nuclear Overhauser enhancement and exchange cross-peaks are indicated by *arrows*. Diagonal peaks of Thr (*T6*) and Lys (*K8*) amide protons from the phosphorylated Thr-187 peptides are identified by *arrows*. *D* and *E*, ratios of cross-peak and diagonal peak intensities for the *cis* and *trans* conformations of Thr-6 on rotating frame nuclear Overhauser enhancement mixing times and its isomerization rates are indicated; *D*, from the *cis* to *trans* (k_{ct}^{cat}) conformation; *E*, from the *trans* to *cis* (k_{tc}^{cat}) conformation. *F*, illustration of the conformational change of phosphorylated Thr-187 peptides by Pin1. The peptide models were generated using PyMOL. In the absence of Pin1, the isomerization rates between the *cis* and *trans* conformations are very slow; however, in the presence of Pin1, the isomerization rates are greatly enhanced by Pin1. The rates of Thr-6 are presented.

Pin1 Plays a Role in the Ubiquitination of p27^{Kip1}—To further explore the molecular mechanisms underlying Pin1 regulation of p27^{Kip1} stability, we evaluated whether Pin1 is in fact involved in the p27^{Kip1} ubiquitination machinery. To this end, we performed *in vivo* ubiquitination assays in which following the treatment of MG132, FLAG-p27^{Kip1} and Myc-ubiquitin proteins were co-immunoprecipitated from Pin1-WT and -KO MEF cell lysates, respectively. Western blotting analyses revealed that p27^{Kip1} is strongly polyubiquitinated in Pin1-KO MEFs but only modestly so in Pin1-WT MEFs (Fig. 5*A*). To rule out the possibility that the polyubiquitination bands detected were not because of a contamination by the polyubiquitinated p27^{Kip1}-associated proteins, we performed a reciprocal pulldown experiment by co-expressing the FLAG-ubiquitin and GFP-p27^{Kip1} in Pin1-WT and KO MEF cells. Consistent with previous results shown in Fig. 5*A*, loss of Pin1 significantly enhanced the polyubiquitination of p27^{Kip1} (Fig. 5*B*). These results are in a good agreement with our previous findings that in the presence of Pin1, p27^{Kip1} protein accumulates at a higher level (Fig. 4*A* and supplemental Fig. S2), whereas in the absence of Pin1, the half-life of p27^{Kip1} is much shorter because of a more rapid degradation rate (Fig. 4*C*).

The crystallographic structure of Skp2-Cks1-p27^{Kip1} complex shows that Cks1 directly binds to the phosphorylated Thr-187 site in p27^{Kip1} and promotes its degradation (15). On the other hand, we find in our present study that Pin1 enhances p27^{Kip1} stability also through the phosphorylated Thr-187. Given that these two proteins bind to the same site on p27^{Kip1} but exert an opposite effect, we hypothesized that Pin1 might compete with Cks1 for binding to p27^{Kip1}. To test this hypothesis, a gradient concentration of recombinant human Pin1 proteins was added to co-immunoprecipitation lysates in which FLAG-p27^{Kip1}-T187D (a mutant that mimics the phosphorylated-Thr-187 of p27^{Kip1}) and HA-Cks1 were co-overexpressed. As shown in Fig. 5*C*, a lower level of Cks1 remains bound to p27^{Kip1} in the presence of a higher concentration of Pin1, suggesting that Pin1 competes with Cks1 for binding to p27^{Kip1}. Moreover, we fur-

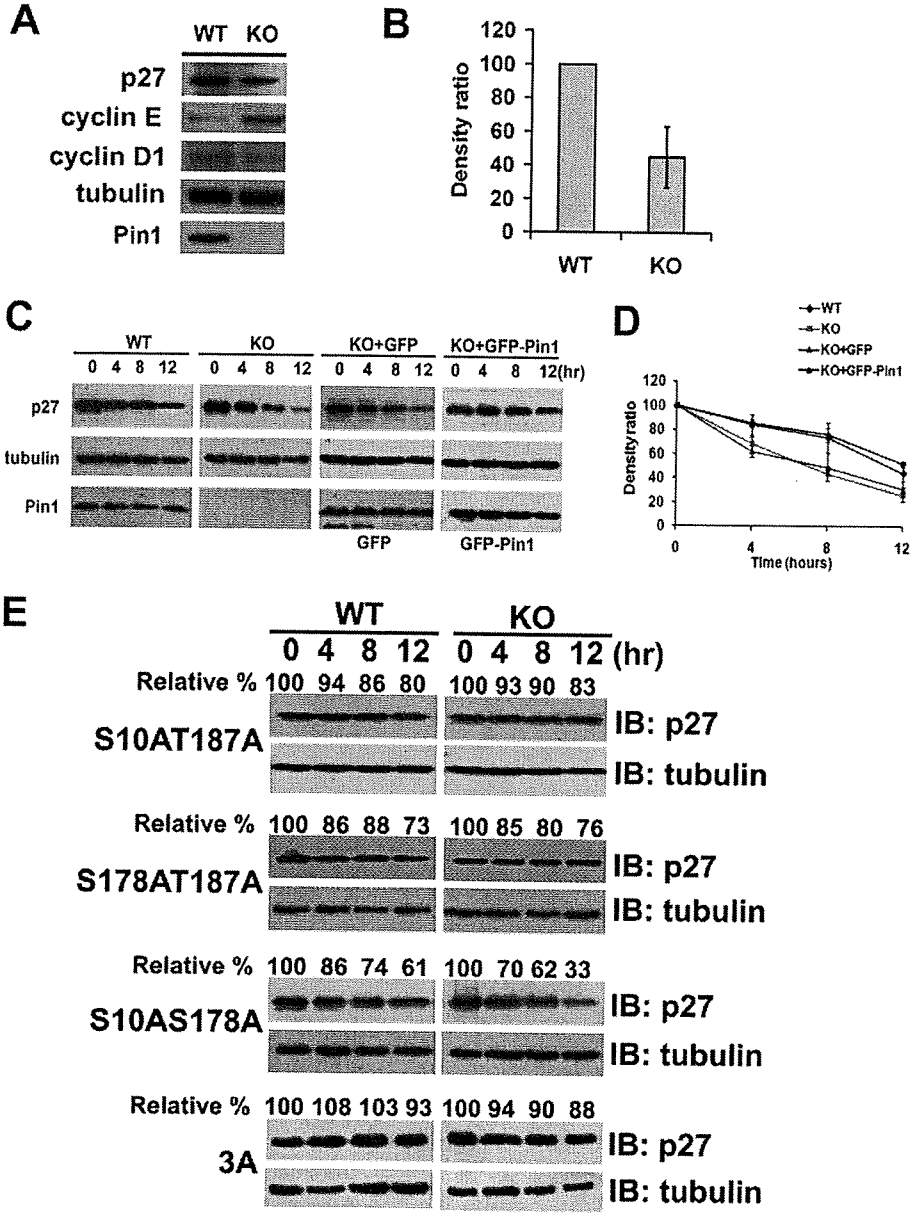

FIGURE 4. **Pin1 regulates p27^{Kip1} stability.** *A*, immunoblotting analysis of the endogenous p27^{Kip1}, cyclin E, and cyclin D1 levels in Pin1-WT and -KO MEFs. *B*, quantification of endogenous p27^{Kip1} levels shown in *A*, normalized to tubulin levels. *C*, protein stability assay of endogenous p27^{Kip1} in both Pin1-WT and -KO MEFs. Cells were starved for 36 h before their arrest at G_0 phase. The cells were then treated with cycloheximide, harvested at 4-h intervals (*left panel*), and analyzed by immunoblotting. To confirm the function of Pin1 in regulating p27^{Kip1} stability, GFP-Pin1 and GFP vectors were re-introduced into Pin1-KO MEF cells, respectively, followed by a protein stability assay. *D*, densitometric analysis of the degradation assays from *C*, normalized to tubulin levels. *E*, protein stability assay of exogenous FLAG-p27^{Kip1} or its mutants in either Pin1-WT or -KO MEFs. Cells were treated with cycloheximide after 24 h of transfection and then harvested at 4-h intervals, followed by immunoblotting (*IB*) analyses. Tubulin was used as a loading control. *KO*, knock-out.

ther confirmed this observation *in vivo* by co-overexpressing FLAG-p27^{Kip1}-T187D and HA-Cks1 in Pin1-WT and -KO MEFs. Our co-immunoprecipitation results show that a markedly higher level of Cks1 is precipitated by p27^{Kip1} in the Pin1-null background compared with the WT background (Fig. 5*D*), suggesting that the interaction of p27^{Kip1} with Cks1 is significantly impaired in the presence of Pin1. Collectively, however, our results illustrate that Pin1 stabilizes p27^{Kip1}, possibly due to its inhibition of the association of Cks1 with p27^{Kip1}.

DISCUSSION

We report herein that Pin1 plays a protective role during the turnover of p27^{Kip1} in a phosphorylation-dependent manner. We describe a novel molecular mechanism by which Pin1 alters the conformation of phosphorylated p27^{Kip1}, thereby suppressing the association of Cks1 and p27^{Kip1} and preventing p27^{Kip1} degradation via the SCF complex (Fig. 6). Our study thus sheds new light on the biological function of Pin1 as an important regulator of specific protein abundance and also uncovers evidence of a cross-talk between post-phosphorylation regulation and the ubiquitination-mediated degradation of proteins.

Pin1 provides a novel mechanism for p27^{Kip1} ubiquitin-proteasome degradation. It has been extensively shown that the degradation of p27^{Kip1} is regulated by its subcellular compartmentalization (11, 42), phosphorylation status (43–44), and the availability of components in the degradation complex (13–15). In this study, we show that the ubiquitination status of p27^{Kip1} is noticeably increased in the absence of Pin1, indicating that the role of Pin1 is significant in regulating this process. Our NMR studies clearly show that the phosphorylated p27^{Kip1} undergoes a conformational change mediated by Pin1, suggesting that the post-phosphorylation modification may be crucial for preventing the recognition of p27^{Kip1} by its degradation machinery. Cks1 is an important factor in p27^{Kip1} degradation (13–15), and we further find that Pin1 disrupts the binding of Cks1 to phosphorylated p27^{Kip1}. Therefore, one of the possible mechanisms could be that the conformational changes of p27^{Kip1} catalyzed by Pin1 is unfavorable for the binding of Cks1, resulting in a reduced interaction of p27^{Kip1} with the SCF complex and an enhancement of p27^{Kip1} stability (Figs. 5 and 6). From the structure of Skp1-Skp2-Cks1-p27^{Kip1} complex, we further found that Cks1 indeed interacts with a *trans* conformation of the Thr-187-Pro motif in p27^{Kip1} (15), suggesting

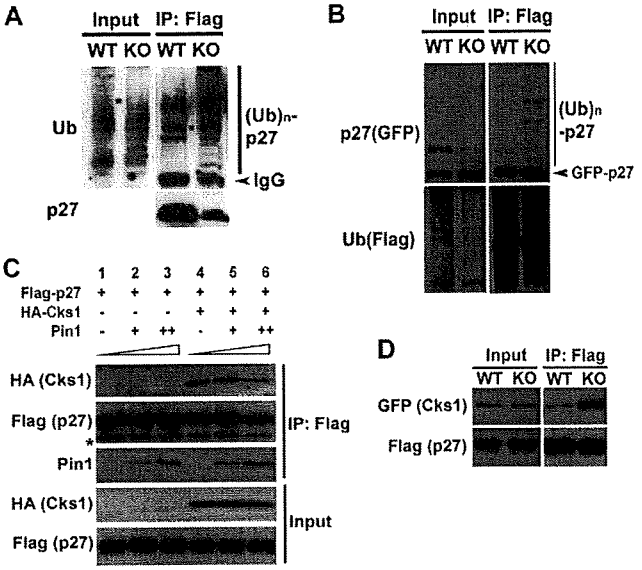

FIGURE 5. **Pin1 is involved in p27^{Kip1} polyubiquitination.** *A, in vivo* ubiquitination (*Ub*) assay of FLAG-p27^{Kip1} in Pin1-WT and -KO MEFs. At 24 h following transfection, cells were treated with 10 μM MG132 to inhibit protein degradation. After 3 h of MG132 treatment, cells were harvested, and lysates were then incubated with FLAG-M2. Western blots were carried out using anti-FLAG or anti-ubiquitin antibody. *IP*, immunoprecipitation; *KO*, knock-out. *B*, reciprocal experiments were carried out as in *A*, after FLAG beads pulldown, and the beads were cooked at 95 °C for 5 min, and Western blots were done by blotting with either anti-p27^{Kip1} or anti-ubiquitin antibody. *C*, effects of Pin1 on co-immunoprecipitation of HA-Cks1 and FLAG-p27^{Kip1}. Immunoblotting analysis of HA-Cks1 bound to FLAG-p27^{Kip1} in the presence of different concentrations of recombinant Pin1 protein are shown. *D*, co-immunoprecipitation of HA-Cks1 and FLAG-p27^{Kip1} in the presence or absence of Pin1. Immunoblotting analysis of HA-Cks1 bound to FLAG-p27^{Kip1} in Pin1-WT and -KO MEFs, respectively, is shown.

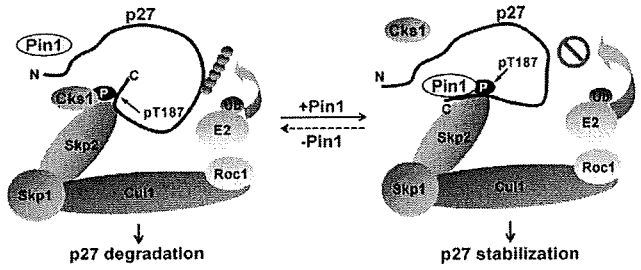

FIGURE 6. **A putative mechanism for Pin1 in the regulation of p27^{Kip1}.** Cks1 binds to phosphorylated p27^{Kip1} and promotes its degradation through ubiquitination (*Ub*). However, to regulate p27^{Kip1} stability at specific time points, Pin1 binds phosphorylated p27^{Kip1} and catalyzes its conformational change, which hinders the association of p27^{Kip1} with Cks1. This process in turn inhibits the polyubiquitination and degradation of p27^{Kip1}.

that Cks1 may have a structural preference to its target. In the presence of Pin1, the *cis-trans* isomerization rate of Thr-187-Pro motif is increased by more than 10-fold. This result suggests that the conformational change catalyzed by Pin1 is a critical regulatory mechanism in mediating the interaction of Cks1 and p27^{Kip1}. Another possible mechanism could be that the Pin1 enhances the dephosphorylation of p27^{Kip1} by its downstream phosphatase, resulting in a reduction of the binding to Cks1 and rescuing p27^{Kip1} stability. It has been reported that Pin1 can regulate the conformation and dephosphorylation of its substrates (25, 29). Pin1 facilitates the dephosphorylation of Cdc25 and Tau by PP2A, a conformation-specific proline-directed phosphatase that effectively dephosphorylates only the *trans*-Ser/Thr-Pro motifs (29). It would be interesting to further investigate whether Pin1 can regulate the dephosphorylation of p27^{Kip1} in the future. The third possible mechanism is that Pin1 competes with Cks1 or other components of the SCF complex for binding to phosphorylated p27^{Kip1} (Figs. 5 and 6). Indeed, we also find that GST-Pin1 can pulldown Skp2 *in vitro* (data not shown), indicating that Pin1 may become incorporated into the p27^{Kip1} degradation complex and is likely to have a regulatory role. Our current study provides the first experimental evidence of a novel "post-phosphorylation" regulation mechanism for the polyubiquitination of p27^{Kip1}. Therefore, overall the post-phosphorylation mechanisms mediated by prolyl isomerases may be a crucial determinant of the abundance of some proteins such as β-catenin (18), cyclin D1 (21), and NF-κB (24) *in vivo*.

There are three Ser/Thr-Pro motifs on p27^{Kip1}, Ser-10, Ser-178, and Thr-187, which are potential Pin1-binding sites. Among these, Thr-187 is the most well characterized site for p27^{Kip1} degradation, as revealed in a number of previous studies (13, 40, 45). Using peptide chips and co-immunoprecipitation assays, our current results further indicate that phosphorylated Thr-187 of p27^{Kip1} is the most favored Pin1-binding site. At the same time, we also find that this interaction is fully abolished only when all three of these Ser/Thr-Pro sites are mutated, indicating that all Ser/Thr-Pro motifs, at least partially, might be involved in the Pin1-p27^{Kip1} interaction. Although Ser-10 is reported to be the major phosphorylated site in p27^{Kip1} (6, 7), our stability assay shows that the stability of S178A/T187A mutant has no significant difference in Pin1-WT and -KO MEF cells (Fig. 4*E*), suggesting that the interaction of Pin1 with phosphorylated Ser-10 may not have a significant effect on p27^{Kip1} stability. On the other hand, because Pin1 can associate both sites, it would also be interesting to test whether Pin1 can induce conformational changes on Ser(P)-10 or Ser(P)-178 peptides in the future. In addition, FOXO4 is known to regulate the p27^{Kip1} level through transcriptional regulation. Recently, it was reported that the overexpression of Pin1 inhibits FOXO4 transcriptional activity resulting in an impairment of p27^{Kip1} expression (46). To confirm this, we also tested the turnover rate of p27^{Kip1} in HEK 293T cells with or without ectopically overexpressed Pin1 (supplemental Fig. S2), but we observed no ectopic effects of Pin1 on p27^{Kip1} stability. However, because of a high endogenous level of Pin1 in HEK 293T cells, additional ectopic expression may not have significant effects, similar to the results shown previously (46). On the other hand, we show that the loss of Pin1 in cells significantly enhances the polyubiquitination levels of p27^{Kip1} resulting in reduced stability (Fig. 4, *A* and *C*). Furthermore, we also demonstrated that there is little or no detectable FOXO4 in our MEFs (supplemental Fig. S3), suggesting the regulatory function of Pin1 on p27^{Kip1} degradation is not likely to be mediated through FOXO4 in our study.

Isomerization of the phosphorylated Ser/Thr-Pro motifs by Pin1 is a key mechanism underlying a post-phosphorylation regulation in many proteins. In general, Pin1 catalyzes the conformational changes of its substrates and thereby alters their properties, *e.g.* transcriptional activity, protein-protein interac-

tion, and subcellular localization. The *cis-trans* isomerization of proline is thus likely to be a key regulatory switch in signal transduction. Given the cumulative evidence to date, we also propose that by switching the *cis-trans* conformations of the proline residue, Pin1 plays a pivotal role in the protein degradation machinery. For instance, Pin1 stabilizes cyclin D1 (21), NF-κB (24), β-catenin (18), p53 (22, 23), p73 (47), and Tax (48). On the other hand, Pin1 negatively regulates protein stability, including that of c-Myc (49), SRC-3 (50), IRF3 (51), cyclin E (41), Daxx (52), and SMRT (53). Additionally, many of these substrates undergo ubiquitination-mediated proteosomal degradation. The turnover of Pin1 substrates is generally through the *cis-trans* conformational changes. In this study, we report that Pin1 stabilizes p27^{Kip1} by a direct involvement in its degradation machinery, which adds weight to a general role for Pin1 in regulating protein stability. Hence, the post-phosphorylation isomerization by Pin1 may act as a molecular switch that determines the fate of its substrates. However, the reason why Pin1 can act as both a stabilizer and a de-stabilizer is unclear at present. Future studies focusing on the general function of Pin1 in ubiquitination-mediated protein degradation may help to elucidate this issue.

The molecular mechanisms underlying the regulation of p27^{Kip1} by Pin1 are likely to be highly complex given the roles that both proteins play in different phases of the cell cycle. As an example of this, the overexpression of Pin1 in mammalian cells leads to a G_2 arrest, whereas its inhibition causes mitotic arrest (16). Moreover, Pin1 regulates the turnover of c-Myc and cyclin E (49, 41), both of which play critical roles in the G_1/S phase transition, and the cyclin E protein has been shown to be further destabilized by Pin1 in MEFs (41). On the other hand, we have also reported that Pin1 can regulate cyclin D1 through both transcriptional and translational mechanisms (17–18, 21). Pin1 directly stabilizes cyclin D1 and regulates its localization; in the absence of Pin1, the cyclin D1 protein levels are markedly reduced (21). Furthermore, the cell cycle reentry of Pin1-KO MEFs is retarded in response to serum starvation (55). Taken together, these results suggest that Pin1 plays a pivotal role in the G_0/G_1-S transition. You *et al.* (56) have reported in their previous study that in response to IGF-1 treatment, Pin1-KO MEFs display a delayed entry into S phase. Conversely, IGF-1 was found to stimulate Pin1 expression, resulting in an increased expression of cyclin D1 and the phosphorylation of pRb, thus further promoting the G_0/G_1-S transition (56). The transcription factor E2F is known to be regulated by pRb, the hyperphosphorylation of which releases E2F1 thereby activating the downstream essential genes for the G_1/S phases of the cell cycle. In addition, E2F1 cannot only bind to the p27^{Kip1} promoter (57), but also the Pin1 promoter (58) and activates the expression of these two proteins. On the other hand, the Cdk inhibitor p27^{Kip1} can prevent pRb phosphorylation by inhibiting the activities of cyclin D1/Cdk4 and cyclin E/Cdk2 (59, 60). Interestingly, the phosphorylation of Thr-187 on p27^{Kip1} by cyclin E/Cdk2 and the subsequent recognition by the ubiquitin ligase Skp2 SCF proteasome complex are the predominant mechanisms that regulate the protein abundance of p27^{Kip1}. In this study, we show that the phosphorylation-dependent ubiquitination of p27^{Kip1} is highly controlled by Pin1, further highlighting the complexity of the cell cycle regulatory processes in which Pin1 and p27^{Kip1} function.

Interestingly and unexpectedly, Pin1 knock-out mice are viable and undergo relatively normal development despite several age-dependent and cell-proliferative abnormalities (21). Accordingly, Pin1-KO MEFs are slightly slower growing than their wild-type counterparts but otherwise show no significant differences. Conversely, overexpression of Pin1 not only confers transforming properties on epithelial cells but also enhances the transformed phenotypes of Neu/Ras activated mammary epithelial cells, indicating an important role of Pin1 in tumor formation (58). On the other hand, it is also surprising that the inactivation of the Thr-187-dependent p27^{Kip1} turnover pathway has no severe impact on cell cycle regulation, as revealed by studies of p27^{Kip1}T187A knock-in mice. In addition, these mice are viable and display only modest cell-proliferative alterations (61). More interestingly, the p27^{Kip1}Thr-187A can also be down-regulated in activated K-*ras*-induced lung tumors, and the p27^{Kip1}Thr-187A mice have a same tumor-dependent death rate as the p27^{Kip1} wild-type mice, implying that an alternative degradation pathway other than Skp2-dependent mechanism plays a significant role in regulating p27^{Kip1} stability (54). Taken together, these observations suggest, at least in part, that there are negative feedback mechanisms in different phases of the cell cycle that control p27^{Kip1} degradation and Pin1 isomerase activity. Given our current data showing that Pin1 also interacts with and stabilizes p27^{Kip1}, further studies of the temporal and spatial regulation of phosphorylated p27^{Kip1} mediated by Pin1 may provide a better understanding of cell cycle control. Also, it would be interesting to cross Pin1 knock-out mice with cyclin D1, cyclin E, or p27^{Kip1} transgenic/knock-out mice to dissect each of their roles in this complicated cell cycle progression.

In conclusion, our current study elucidates a novel molecular mechanism by which phosphorylated p27^{Kip1} is further regulated by the peptidylprolyl isomerase Pin1. This may underscore the significance of prolyl isomerization in the post-phosphorylation regulation and polyubiquitination-directed degradation of proteins in the cell.

Acknowledgments—We thank K. P. Lu for providing invaluable Pin1 antibody, plasmids, and MEFs. We also thank H. Y. Sun and C. Lu for peptide synthesis and technical assistance with the peptide arrays. We also thank the anonymous reviewers for their invaluable comments. We are grateful to the members of Y. C. Liou laboratory for useful discussions and to K. Perrem, B. L. Tan, and B. C. Low for excellent advice during the preparation of the manuscript.

REFERENCES

1. Borriello, A., Cucciolla, V., Oliva, A., Zappia, V., and Della Ragione, F. (2007) *Cell Cycle* **6**, 1053–1061
2. Reed, S. I. (2002) *Cell Cycle* **1**, 389–390
3. Viglietto, G., Motti, M. L., and Fusco, A. (2002) *Cell Cycle* **1**, 394–400
4. Sherr, C. J., and Roberts, J. M. (1999) *Genes Dev.* **13**, 1501–1512
5. Kaldis, P. (2007) *Cell* **26**, 241–244
6. Vervoorts, J., and Lüscher, B. (2008) *Cell. Mol. Life Sci.* **65**, 3255–3264
7. Ishida, N., Kitagawa, M., Hatakeyama, S., and Nakayama, K. (2000) *J. Biol. Chem.* **275**, 25146–25154
8. Nguyen, L., Besson, A., Heng, J. I., Schuurmans, C., Teboul, L., Parras, C.,

Philpott, A., Roberts, J. M., and Guillemot, F. (2006) *Genes Dev.* **20,** 1511–1524
9. Baldassarre, G., Belletti, B., Nicoloso, M. S., Schiappacassi, M., Vecchione, A., Spessotto, P., Morrione, A., Canzonieri, V., and Colombatti, A. (2005) *Cancer Cell* **7,** 51–63
10. McAllister, S. S., Becker-Hapak, M., Pintucci, G., Pagano, M., and Dowdy, S. F. (2003) *Mol. Cell. Biol.* **23,** 216–228
11. Rodier, G., Montagnoli, A., Di Marcotullio, L., Coulombe, P., Draetta, G. F., Pagano, M., and Meloche, S. (2001) *EMBO J.* **20,** 6672–6682
12. Kotake, Y., Nakayama, K., Ishida, N., and Nakayama, K. I. (2005) *J. Biol. Chem.* **280,** 1095–1102
13. Ganoth, D., Bornstein, G., Ko, T. K., Larsen, B., Tyers, M., Pagano, M., and Hershko, A. (2001) *Nat. Cell Biol.* **3,** 321–324
14. Seeliger, M. A., Breward, S. E., Friedler, A., Schon, O., and Itzhaki, L. S. (2003) *Nat. Struct. Biol.* **10,** 718–724
15. Hao, B., Zheng, N., Schulman, B. A., Wu, G., Miller, J. J., Pagano, M., and Pavletich, N. P. (2005) *Mol. Cell* **20,** 9–19
16. Lu, K. P., Hanes, S. D., and Hunter, T. (1996) *Nature* **380,** 544–547
17. Wulf, G. M., Ryo, A., Wulf, G. G., Lee, S. W., Niu, T., Petkova, V., and Lu, K. P. (2001) *EMBO J.* **20,** 3459–3472
18. Ryo, A., Nakamura, M., Wulf, G., Liou, Y. C., and Lu, K. P. (2001) *Nat. Cell Biol.* **3,** 793–801
19. Shen, Z. J., Esnault, S., Schinzel, A., Borner, C., and Malter, J. S. (2009) *Nat. Immunol.* **10,** 257–265
20. Rustighi, A., Tiberi, L., Soldano, A., Napoli, M., Nuciforo, P., Rosato, A., Kaplan, F., Capobianco, A., Pece, S., Di Fiore, P. P., and Del Sal, G. (2009) *Nat. Cell Biol.* **11,** 133–142
21. Liou, Y. C., Ryo, A., Huang, H. K., Lu, P. J., Bronson, R., Fujimori, F., Uchida, T., Hunter, T., and Lu, K. P. (2002) *Proc. Natl. Acad. Sci. U.S.A.* **99,** 1335–1340
22. Zacchi, P., Gostissa, M., Uchida, T., Salvagno, C., Avolio, F., Volinia, S., Ronai, Z., Blandino, G., Schneider, C., and Del Sal, G. (2002) *Nature* **419,** 853–857
23. Zheng, H., You, H., Zhou, X. Z., Murray, S. A., Uchida, T., Wulf, G., Gu, L., Tang, X., Lu, K. P., and Xiao, Z. X. (2002) *Nature* **419,** 849–853
24. Ryo, A., Suizu, F., Yoshida, Y., Perrem, K., Liou, Y. C., Wulf, G., Rottapel, R., Yamaoka, S., and Lu, K. P. (2003) *Mol. Cell* **12,** 1413–1426
25. Liou, Y. C., Sun, A., Ryo, A., Zhou, X. Z., Yu, Z. X., Huang, H. K., Uchida, T., Bronson, R., Bing, G., Li, X., Hunter, T., and Lu, K. P. (2003) *Nature* **424,** 556–561
26. Pastorino, L., Sun, A., Lu, P. J., Zhou, X. Z., Balastik, M., Finn, G., Wulf, G., Lim, J., Li, S. H., Li, X., Xia, W., Nicholson, L. K., and Lu, K. P. (2006) *Nature* **440,** 528–534
27. Ryo, A., Togo, T., Nakai, T., Hirai, A., Nishi, M., Yamaguchi, A., Suzuki, K., Hirayasu, Y., Kobayashi, H., Perrem, K., Liou, Y. C., and Aoki, I. (2006) *J. Biol. Chem.* **281,** 4117–4125
28. Lim, J., Balastik, M., Lee, T. H., Nakamura, K., Liou, Y. C., Sun, A., Finn, G., Pastorino, L., Lee, V. M., and Lu, K. P. (2008) *J. Clin. Invest.* **118,** 1877–1889
29. Lu, K. P., and Zhou, X. Z. (2007) *Nat. Rev. Mol. Cell Biol.* **8,** 904–916
30. Takahashi, K., Uchida, C., Shin, R. W., Shimazaki, K., and Uchida, T. (2008) *Cell. Mol. Life Sci.* **65,** 359–375
31. Yeh, E. S., and Means, A. R. (2007) *Nat. Rev. Cancer* **7,** 381–388
32. Shaw, P. E. (2007) *EMBO Rep.* **8,** 40–45
33. Ryo, A., Wulf, G., Lee, T. H., and Lu, K. P. (2009) *Trends Biochem. Sci.* **34,** 162–165
34. Bax, A., and Davis, D. G. (1985) *J. Magn. Reson.* **63,** 207–213
35. Bax, A., and Davis, D. G. (1985) *J. Magn. Reson.* **65,** 355–360
36. Yaffe, M. B., Schutkowski, M., Shen, M., Zhou, X. Z., Stukenberg, P. T., Rahfeld, J. U., Xu, J., Kuang, J., Kirschner, M. W., Fischer, G., Cantley, L. C., and Lu, K. P. (1997) *Science* **278,** 1957–1960
37. Lu, P. J., Zhou, X. Z., Liou, Y. C., Noel, J. P., and Lu, K. P. (2002) *J. Biol. Chem.* **277,** 2381–2384
38. Stiffler, M. A., Chen, J. R., Grantcharova, V. P., Lei, Y., Fuchs, D., Allen, J. E., Zaslavskaia, L. A., and MacBeath, G. (2007) *Science* **317,** 364–369
39. Sun, H., Lu, C. H., Uttamchandani, M., Xia, Y., Liou, Y. C., and Yao, S. Q. (2008) *Angew. Chem. Int. Ed. Engl.* **47,** 1698–1702
40. Sheaff, R. J., Groudine, M., Gordon, M., Roberts, J. M., and Clurman, B. E. (1997) *Genes Dev.* **11,** 1464–1478
41. Yeh, E. S., Lew, B. O., and Means, A. R. (2006) *J. Biol. Chem.* **281,** 241–251
42. Connor, M. K., Kotchetkov, R., Cariou, S., Resch, A., Lupetti, R., Beniston, R. G., Melchior, F., Hengst, L., and Slingerland, J. M. (2003) *Mol. Biol. Cell* **14,** 201–213
43. Liang, J., Zubovitz, J., Petrocelli, T., Kotchetkov, R., Connor, M. K., Han, K., Lee, J. H., Ciarallo, S., Catzavelos, C., Beniston, R., Franssen, E., and Slingerland, J. M. (2002) *Nat. Med.* **8,** 1153–1160
44. Shin, I., Yakes, F. M., Rojo, F., Shin, N. Y., Bakin, A. V., Baselga, J., and Arteaga, C. L. (2002) *Nat. Med.* **8,** 1145–1152
45. Kossatz, U., Dietrich, N., Zender, L., Buer, J., Manns, M. P., and Malek, N. P. (2004) *Genes Dev.* **18,** 2602–2607
46. Brenkman, A. B., de Keizer, P. L., van den Broek, N. J., van der Groep, P., van Diest, P. J., van der Horst, A., Smits, A. M., and Burgering, B. M. (2008) *Cancer Res.* **68,** 7597–7605
47. Mantovani, F., Piazza, S., Gostissa, M., Strano, S., Zacchi, P., Mantovani, R., Blandino, G., and Del Sal, G. (2004) *Mol. Cell* **14,** 625–636
48. Jeong, S. J., Ryo, A., and Yamamoto, N. (2009) *Biochem. Biophys. Res. Commun.* **381,** 294–299
49. Yeh, E., Cunningham, M., Arnold, H., Chasse, D., Monteith, T., Ivaldi, G., Hahn, W. C., Stukenberg, P. T., Shenolikar, S., Uchida, T., Counter, C. M., Nevins, J. R., Means, A. R., and Sears, R. (2004) *Nat. Cell Biol.* **6,** 308–318
50. Yi, P., Wu, R. C., Sandquist, J., Wong, J., Tsai, S. Y., Tsai, M. J., Means, A. R., and O'Malley, B. W. (2005) *Mol. Cell. Biol.* **25,** 9687–9699
51. Saitoh, T., Tun-Kyi, A., Ryo, A., Yamamoto, M., Finn, G., Fujita, T., Akira, S., Yamamoto, N., Lu, K. P., and Yamaoka, S. (2006) *Nat. Immunol.* **7,** 598–605
52. Ryo, A., Hirai, A., Nishi, M., Liou, Y. C., Perrem, K., Lin, S. C., Hirano, H., Lee, S. W., and Aoki, I. (2007) *J. Biol. Chem.* **282,** 36671–36681
53. Stanya, K. J., Liu, Y., Means, A. R., and Kao, H. Y. (2008) *J. Cell Biol.* **183,** 49–61
54. Timmerbeul, I., Garrett-Engele, C. M., Kossatz, U., Chen, X., Firpo, E., Grünwald, V., Kamino, K., Wilkens, L., Lehmann, U., Buer, J., Geffers, R., Kubicka, S., Manns, M. P., Porter, P. L., Roberts, J. M., and Malek, N. P. (2006) *Proc. Natl. Acad. Sci. U.S.A.* **103,** 14009–14014
55. Fujimori, F., Takahashi, K., Uchida, C., and Uchida, T. (1999) *Biochem. Biophys. Res. Commun.* **265,** 658–663
56. You, H., Zheng, H., Murray, S. A., Yu, Q., Uchida, T., Fan, D., and Xiao, Z. X. (2002) *J. Cell. Biochem.* **84,** 211–216
57. Wang, C., Hou, X., Mohapatra, S., Ma, Y., Cress, W. D., Pledger, W. J., and Chen, J. (2005) *J. Biol. Chem.* **280,** 12339–12343
58. Ryo, A., Liou, Y. C., Wulf, G., Nakamura, M., Lee, S. W., and Lu, K. P. (2002) *Mol. Cell. Biol.* **22,** 5281–5295
59. Cheng, M., Olivier, P., Diehl, J. A., Fero, M., Roussel, M. F., Roberts, J. M., and Sherr, C. J. (1999) *EMBO J.* **18,** 1571–1583
60. Sherr, C. J., and Roberts, J. M. (2004) *Genes Dev.* **18,** 2699–2711
61. Malek, N. P., Sundberg, H., McGrew, S., Nakayama, K., Kyriakides, T. R., Roberts, J. M., and Kyriakidis, T. R. (2001) *Nature* **413,** 323–327

Research Focus

Pinning down HER2–ER crosstalk in SMRT regulation

Akihide Ryo[1], Gerburg Wulf[2], Tae Ho Lee[2] and Kun Ping Lu[2]

[1] AIDS Research Center, National Institute of Infectious Diseases, 1-23-1 Toyama, Shinjuku-ku, Tokyo 162-8640, Japan
[2] Department of Medicine, Beth Israel Deaconess Medical Center, Harvard Medical School, 330 Brookline Avenue, CLS0408, Boston, MA 02215, USA

SMRT (silencing mediator for retinoic acid and thyroid hormone receptors) is a transcriptional co-repressor that mediates the repressive function of nuclear hormone receptors such as the estrogen receptor (ER). Decreased SMRT levels correlate with acquired tamoxifen resistance in breast cancer, and SMRT restoration might resensitize breast cancer cells to tamoxifen. A new study demonstrates that SMRT protein stability is regulated by phosphorylation-dependent Pin1-catalyzed prolyl-isomerization. Pin1 functions downstream of HER2, positioning it as an important modulator of the crosstalk between ER and growth factor signaling.

Breast cancer and the estrogen receptor

Breast cancer is one of the most common malignancies in women and the second most common cause of female cancer-related deaths [1]. However, deaths due to breast cancer have decreased in recent years owing to the development of targeted therapies, including hormone therapy, in addition to conventional chemotherapy and surgical interventions [1]. The majority of breast cancers in post-menopausal women express the estrogen receptor (ER), and after surgery they can be treated with hormonal therapy alone, in the absence of more toxic chemotherapy, resulting in a relatively favorable prognosis [2]. However, a significant fraction of these hormone-sensitive breast cancer patients will experience disease progression that is attributable to the resistance to endocrine agents, such as tamoxifen, thus resulting in mortality [3]. Therefore, it is desirable to develop new strategies to treat hormone refractory breast cancer; this goal will probably be facilitated by elucidating the underlying molecular mechanisms of hormone resistance. A new study by Stanya and colleagues [4] delineates an important hint in solving the riddle of endocrine resistance. They find that Cdk2 (cyclin dependent kinase 2)-mediated phosphorylation of SMRT (silencing mediator for retinoid and thyroid receptors), an ER co-repressor, creates binding sites for protein (peptidyl-prolyl cis/trans isomerase) NIMA-interacting 1 (Pin1), which in turn induces conformational changes to promote SMRT degradation (Figure 1a). Moreover, this event crucially mediates human epidermal growth factor receptor 2 (HER2)-dependent SMRT protein degradation and resultant endocrine resistance. These findings shed new light on the molecular mechanism of SMRT regulation and warrant further investigation of the role and therapeutic potential of Pin1 in the treatment of endocrine-resistant breast cancers.

ER regulation

ER is a member of the nuclear hormone receptor family, which has important roles in cell proliferation, differentiation and oncogenesis [5]. In response to the hormone estrogen, ER can recruit steroid receptor coactivator-3 (SRC-3; also called amplified in breast cancer-1, AIB1) to enhance estrogen-dependent transcriptional gene activation. In the absence of 17β-estradiol (E2), ER can interact with co-repressors such as SMRT and N-CoR (nuclear receptor co-repressor) to repress target gene expression [6]. Although both SMRT and N-CoR mediate the most repressive function of unliganded ER by recruiting histone deacetylase 3 (HDAC3), only SMRT inhibition is sufficient to de-sensitize cells to tamoxifen-mediated inhibition of ER-induced gene expression [7].

Crosstalk between HER2 and ER

HER2 (also known as ErbB2, ERBB2 and Neu) is a member of the epidermal growth factor receptor family that has a notable role in breast cancer pathogenesis; it is the target of the anti-breast-cancer drug trastuzumab [8]. Both preclinical and clinical evidence implicates HER2 overexpression in the development of endocrine resistance, especially to tamoxifen [9]. The receptor crosstalk between the ER and growth factor receptors affects ER transcriptional activity. For example, HER2-dependent mitogen-activated protein kinase (MAPK) activation triggers both ER and SRC-3 phosphorylation thereby increasing their transcriptional activity [10,11]. MAPK can also phosphorylate SMRT thereby reducing its binding affinity for transcription factors and enhancing its nuclear export [12]. However, it is unknown whether growth factor signaling modulates co-repressor stability. Several previous reports indicate that estrogen markedly downregulates N-CoR protein levels in ER-positive breast cancer cells without affecting SMRT levels [13]. Therefore, it will be of great importance to elucidate the regulatory mechanism(s) underlying SMRT stability in relation to tamoxifen resistance and growth-factor signaling in breast cancer.

The role of Pin1 in HER2–ER crosstalk

The peptidyl-prolyl isomerase Pin1 is an important regulator in HER2-mediated growth signaling and ER-mediated transcription in breast cancer [14]. Unlike other prolyl isomerases, Pin1 binds to discrete phosphorylated Ser/Thr-Pro motifs in a specific group of proteins and catalyzes their *cis–trans* isomerization to regulate protein

Corresponding author: Ryo, A. (aryo@nih.go.jp); Lu, K.P. (klu@bidmc.harvard.edu).

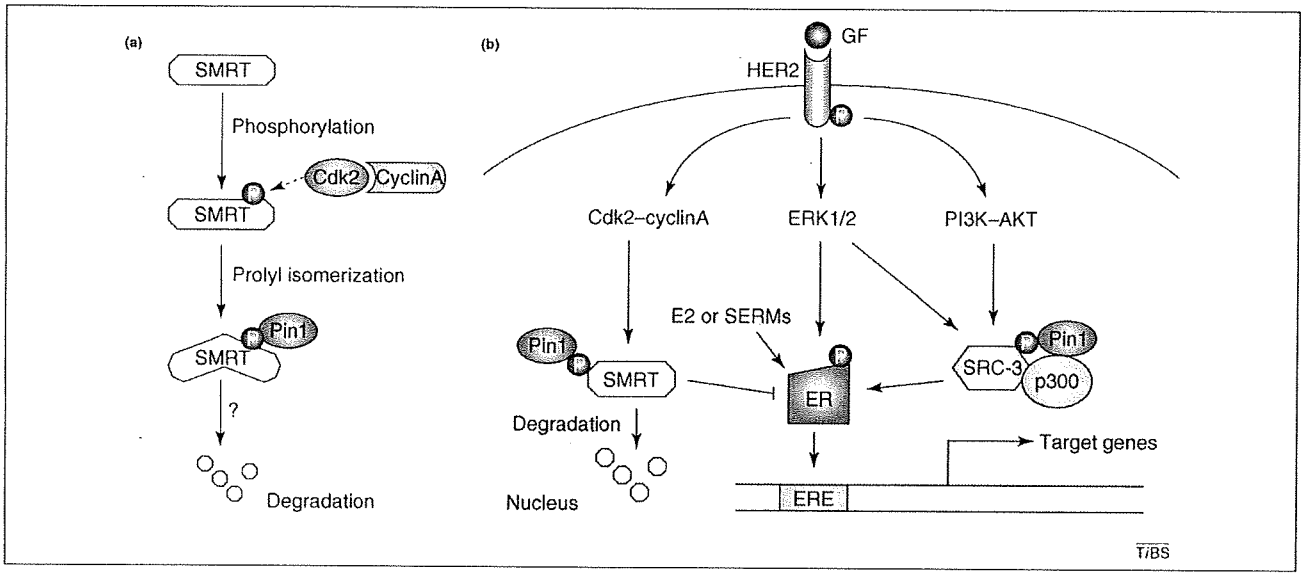

Figure 1. Pin1 functions as a crucial catalyst in the crosstalk between HER2 and ER. **(a)** A novel post-phosphorylation regulatory mechanism for SMRT stability. The phosphorylation of SMRT by the proline-directed kinase Cdk2 (shown with its binding partner, cyclinA) generates binding modules for the prolyl isomerase Pin1. Subsequent prolyl isomerization by Pin1 induces conformational changes and thereby enhances SMRT degradation. **(b)** Pin1 orchestrates signaling cascades from HER2 to ER. Growth-factor-mediated signaling via HER2 activates several downstream kinases, including MAPK (ERK1/2), phosphoinositide 3-kinase (PI3K)–Akt and Cdk2–cyclinA. These kinases, in turn, phosphorylate both the co-repressor SMRT and coactivator SRC-3 (shown in a complex with p300), in addition to ER, creating Pin1-binding sites. Subsequent Pin1-mediated prolyl isomerization activates ER and renders it resistant to SERMs (selective estrogen receptor modulators). These data indicate that Pin1 has a central role in the crosstalk between growth factor signaling and ER during ER-mediated transcription and tamoxifen resistance. GF, growth factor; ERE, estrogen response element.

conformation as a mode of post-phosphorylation regulation. Such Pin1-catalyzed prolyl isomerization can regulate a wide spectrum of phosphorylation-dependent activities, including protein stability [14]. Importantly, Pin1 is highly overexpressed in several human cancers including breast cancer, and its expression levels parallel the malignant properties of many tumors [14,15]. Pin1 is transcriptionally upregulated by the E2F transcription factors in response to growth factors and other stimulating conditions such as HER2 or Ras activation in breast cancer [16]. Moreover, Pin1 inhibition or deletion efficiently suppresses the ability of oncogenic HER2 or Ras to transform normal mammary epithelial cells or to induce breast cancer *in vivo* [16,17]. Thus, Pin1 is essential for growth-factor-induced breast cancer development.

A previous report indicated that Pin1 can regulate SRC-3 activity and turnover [18]. Pin1 binds to phosphorylated SRC-3 and enhances SRC-3-mediated recruitment of cAMP-response-element binding protein (CREB) binding protein (CBP; similar to p300) to the promoters of ER-dependent genes to activate transcription. In addition, Pin1 enhances SRC-3 degradation, an event that seems to promote SRC-3 turnover and sustained activation, rather than its functional attenuation, although a detailed mechanism remains elusive [18]. It remains unclear whether Pin1 can regulate transcriptional co-repressors during and after oncogenesis or whether Pin1 participates in hormone therapy resistance in conjunction with aberrant growth-factor signaling in breast cancers.

Newly identified: Pin1-dependent SMRT regulation

Stanya and colleagues [4] now provide the first evidence that Pin1-catalyzed, phosphorylation-dependent prolyl isomerization promotes SMRT protein degradation, thereby reducing SMRT-mediated ER transcriptional repression. The authors first identified Pin1 as a SMRT interacting partner in a yeast two-hybrid screen, and they confirmed that this interaction relies upon the Pin1 Trp-Trp domain binding phosphorylated SMRT.

One of the functional consequences of the Pin1–SMRT association is to promote SMRT degradation. As Pin1 overexpression compromises SMRT repressor activity, Stanya and colleagues [4] hypothesized that Pin1 might modulate SMRT-mediated repression by affecting its protein stability, as has been shown for other Pin1 targets [14,19]. Indeed, Pin1 overexpression promoted SMRT protein degradation in a dose-dependent manner, whereas Pin1 knockdown or knockout significantly increased SMRT stability. Moreover, the effects of Pin1 knockdown on SMRT stability could be rescued by ectopic Pin1 expression, but not expression of its catalytically inactive mutant [4]. The authors thus concluded that Pin1 regulates SMRT protein half-life.

The authors then mapped the Pin1-binding sites in SMRT via mutational analysis. They also identified multiple Ser and Thr residues in SMRT that are phosphorylated *in vivo*, including two consensus Cdk target sites: Ser1241 and Ser1469. Indeed, Pin1 can interact with SMRT on these two sites *in vitro*. Furthermore, a triple mutant at 3 potential Cdk consensus sites (Ser1241Ala; Thr1445Ala; Ser1469Ala) is neither phosphorylated by Cdk2 nor pulled down by Pin1. Importantly, the SMRT triple mutant is also more stable than wild-type SMRT. In addition, Cdk2 overexpression can reduce exogenous SMRT protein levels, which can be rescued by Pin1 knockdown [4]. Furthermore, siRNA-mediated Cdk2 knockdown

Box 1. Tamoxifen resistance in breast cancer

Tamoxifen is currently the most widely prescribed orally active selective ER modulator for the treatment of breast cancer [21]. Although tamoxifen is an ER antagonist in breast tissue, it has variable cell-type-specific partial agonist or antagonist activities. The antagonist activity enables the drug to block ER-mediated transcription and cancer cell growth in ER-positive breast cancer cells. However, tamoxifen resistance might occur when its agonistic activity overcomes its antagonistic effect [21]. This variability could be related, in part, to the cellular milieu of ER coactivators and co-repressors [10]. For example, increased levels of coactivators, such as SRC-3, enhance the estrogen agonist properties of tamoxifen, whereas decreased levels of co-repressors, such as SMRT and N-CoR, correlate with acquired tamoxifen resistance [9,10]. Therefore, tamoxifen resistance might depend on the relative abundance or activity between co-repressors and coactivators that are often determined by HER2-iniated upstream growth-factor signaling [22].

upregulates endogenous SMRT levels. These data indicate that SMRT phosphorylation by Cdk2 is crucial for Pin1-mediated SMRT degradation.

HER2 signaling can increase Cdk activity and upregulate Pin1 expression in breast cancers [19,20]. Therefore, Stanya and colleagues [4] next explored how ER activity might be regulated by functional crosstalk between HER2 signaling and the Cdk2- and Pin1-dependent SMRT-degradation pathway. A HER2 agonist, for example heregulin, decreases SMRT protein levels, whereas a HER2 inhibitor, for example AG825, increases both SMRT half-life and protein levels. Moreover, Pin1 or Cdk2 knockdown blocks heregulin from decreasing SMRT stability [4]. These data point to HER2 functioning upstream of Cdk2 and Pin1 as a potential regulator of SMRT protein stability.

Finally, to delineate the possible role of the SMRT degradation pathway in tamoxifen resistance (Box 1), the authors investigated the effect of SMRT, Pin1 or Cdk2 knockdown on ER activity after tamoxifen treatment of ER-positive breast cancer cells. They found that tamoxifen treatment represses the expression of two different ER target genes; this effect is compromised by SMRT knockdown. By contrast, Pin1 or Cdk2 knockdown enhances the repression of both ER target genes. Moreover, SMRT knockdown increases cell proliferation, whereas Cdk2 inhibition produces a slight decrease in cell proliferation. Interestingly, Pin1 inhibition does not significantly reduce cell growth despite suppressing ER activity. It thus seems that complex crosstalk between Pin1 or Cdk2 and other proteins involved in cell growth might explain the discrepancy between ER-mediated transcription and cell proliferation on increased SMRT stability.

This new study [4] highlights the potential role for Pin1 as a target for preventing improper ER activation; moreover, it could provide important insight toward understanding the nature of tamoxifen resistance in breast cancer. What remains unclear, however, is the mechanism underlying Pin1-dependent SMRT degradation. The identification of factors involved in the Pin1-mediated SMRT-degradation pathway might uncover vital information regarding the enigmatic cell-type-specific function of Pin1 in SMRT regulation. Furthermore, relevant factors could be potential new therapeutic targets for treating hormone-resistant breast cancers. Because Pin1 can bind to many cellular proteins, it becomes important to ask whether Pin1 fosters ER-mediated transcription and hormone resistance only by decreasing SMRT stability. Indeed, because Pin1 can also increase ER function by acting on SRC-3, it could act together with HER2 signaling as a molecular determinant of the balance between ER co-repression and coactivation (Figure 1b). However, it remains unclear why Pin1-mediated degradation of both the coactivator and co-repressor triggers similar ER activation and how these events are coordinated. Further careful analysis of the interplay between Pin1 and relevant signaling pathways will be necessary to fully delineate the function of Pin1 and its target proteins in the regulation of ER and endocrine resistance in breast cancer.

Concluding remarks

Pin1 regulates both the co-repressor SMRT and the coactivator SRC-3 as a downstream effector of HER2 signaling [4,14,16–18]. Growth-factor-receptor signaling is often increased in endocrine-resistant breast tumors, and it contributes to coactivator upregulation and co-repressor downregulation, thus activating proliferation and/or survival pathways and hormone resistance [9,10]. Interestingly, Pin1 inhibitors (if identified) potentially could be administered to re-sensitize tumors to endocrine therapies. Furthermore, such Pin1 inhibitors could be used along with hormonal therapies to block ER proliferation and/or survival activity and the agonistic effects of selective estrogen receptor modulators such as tamoxifen, which both are often deregulated by aberrant growth factor receptor signaling.

Acknowledgements

Work done in our laboratories is supported by National Institutes of Health grants GM58556, AG17870, AG22082 to K.P.L (www.nih.gov).

References

1 Berry, D.A. *et al.* (2005) Effect of screening and adjuvant therapy on mortality from breast cancer. *N. Engl. J. Med.* 353, 1784–1792
2 Joslyn, S.A. (2002) Hormone receptors in breast cancer: racial differences in distribution and survival. *Breast Cancer Res. Treat.* 73, 45–59
3 Dawood, S. and Cristofanilli, M. (2007) Endocrine resistance in breast cancer: what really matters? *Ann. Oncol.* 18, 1289–1291
4 Stanya, K.J. *et al.* (2008) Cdk2 and Pin1 negatively regulate the transcriptional corepressor SMRT. *J. Cell Biol.* 183, 49–61
5 Parker, M.G. (1993) Steroid and related receptors. *Curr. Opin. Cell Biol.* 5, 499–504
6 Xu, L. *et al.* (1999) Coactivator and corepressor complexes in nuclear receptor function. *Curr. Opin. Genet. Dev.* 9, 140–147
7 Privalsky, M.L. (2004) The role of corepressors in transcriptional regulation by nuclear hormone receptors. *Annu. Rev. Physiol.* 66, 315–360
8 Moasser, M.M. (2007) The oncogene HER2: its signaling and transforming functions and its role in human cancer pathogenesis. *Oncogene* 26, 6469–6487
9 Shou, J. *et al.* (2004) Mechanisms of tamoxifen resistance: increased estrogen receptor-HER2/neu cross-talk in ER/HER2-positive breast cancer. *J. Natl. Cancer Inst.* 96, 926–935
10 Osborne, C.K. *et al.* (2005) Crosstalk between estrogen receptor and growth factor receptor pathways as a cause for endocrine therapy resistance in breast cancer. *Clin. Cancer Res.* 11, 865s–870s
11 Font de Mora, J. and Brown, M. (2000) AIB1 is a conduit for kinase-mediated growth factor signaling to the estrogen receptor. *Mol. Cell. Biol.* 20, 5041–5047

12 Jonas, B.A. and Privalsky, M.L. (2004) SMRT and N-CoR corepressors are regulated by distinct kinase signaling pathways. *J. Biol. Chem.* 279, 54676–54686
13 Frasor, J. *et al.* (2005) Estrogen down-regulation of the corepressor N-CoR: mechanism and implications for estrogen derepression of N-CoR-regulated genes. *Proc. Natl. Acad. Sci. U. S. A.* 102, 13153–13157
14 Lu, K.P. and Zhou, X.Z. (2007) The prolyl isomerase Pin1: a pivotal new twist in phosphorylation signalling and human disease. *Nat. Rev. Mol. Cell Biol.* 8, 904–916
15 Wulf, G.M. *et al.* (2001) Pin1 is overexpressed in breast cancer and potentiates the transcriptional activity of phosphorylated c-Jun towards the cyclin D1 gene. *EMBO J.* 20, 3459–3472
16 Ryo, A. *et al.* (2002) Pin1 is an E2F target gene essential for the Neu/Ras-induced transformation of mammary epithelial cells. *Mol. Cell. Biol.* 22, 5281–5295
17 Wulf, G. *et al.* (2004) Modeling breast cancer *in vivo* and *ex vivo* reveals an essential role of Pin1 in tumorigenesis. *EMBO J.* 23, 3397–3407
18 Yi, P. *et al.* (2005) Peptidyl-prolyl isomerase 1 (Pin1) serves as a coactivator of steroid receptor by regulating the activity of phosphorylated steroid receptor coactivator 3 (SRC-3/AIB1). *Mol. Cell. Biol.* 25, 9687–9699
19 Ryo, A. *et al.* (2001) Pin1 regulates turnover and subcellular localization of β-catenin by inhibiting its interaction with APC. *Nat. Cell Biol.* 3, 793–801
20 Neve, R.M. *et al.* (2000) Effects of oncogenic ErbB2 on G1 cell cycle regulators in breast tumour cells. *Oncogene* 19, 1647–1656
21 Riggs, B.L. and Hartmann, L.C. (2003) Selective estrogen-receptor modulators – mechanisms of action and application to clinical practice. *N. Engl. J. Med.* 348, 618–629
22 Fujita, T. *et al.* (2003) Full activation of estrogen receptor α activation function-1 induces proliferation of breast cancer cells. *J. Biol. Chem.* 278, 26704–26714

0968-0004/$ – see front matter
doi:10.1016/j.tibs.2008.12.004 Available online 9 March 2009